Molecular Recognition of DNA by Rigid [*n*]-Polynorbornane-Derived Bifunctional Intercalators: Synthesis and Evaluation of Their Binding Properties

Liisa D. Van Vliet,[†,‡] Tom Ellis,[†,§] Patrick J. Foley,[||] Ligong Liu,[||] Frederick M. Pfeffer,[⊥] Richard A. Russell,*[,#] Ronald N. Warrener,[||] Florian Hollfelder,*[,‡] and Michael J. Waring*[,§]

Department of Biochemistry, University of Cambridge, 80 Tennis Court Road, Cambridge CB2 1GA, United Kingdom, Department of Pharmacology, University of Cambridge, Tennis Court Road, Cambridge CB2 1PD, United Kingdom, Centre for Molecular Architecture, Central Queensland University, Rockhampton, Australia 4702, School of Biological and Chemical Science, Deakin University, Waurn Ponds, Victoria, Australia 3217, Adelaide Graduate Centre, University of Adelaide, 10 Pulteney St., Adelaide, South Australia 5000

Received November 9, 2006

We have exploited the concept of multivalency in the context of DNA recognition, using novel chemistry to synthesize a new type of bis-intercalator with unusual sequence-selectivity. Bis-intercalation has been observed previously, but design principles for de novo construction of such molecules are not known. Our compounds feature two aromatic moieties projecting from a rigid, polynorbornane-based scaffold. The length and character of the backbone as well as the identity of the intercalators were varied, resulting in mono- or divalent recognition of the double helix with varying affinity. Our lead compound proved to be a moderately sequence-selective bis-intercalator with an unwinding angle of 27° and a binding constant of about 8 μM. 9-Aminoacridine rings were preferred over acridine carboxamides or naphthalimides, and a rigid [3]-polynorbornane scaffold was superior to a [5]-polynorbornane. The flexibility of the linker connecting the rings to the scaffold, although less influential, could affect the strength and character of the DNA binding.

Introduction

Even before the discovery of the double helix, DNA-binding drugs were being used to treat protozoal diseases such as malaria and were widely employed as antiseptics, particularly acridines and their derivatives.[1,2] In addition to acridines, a variety of other substances were commonly used as dyes to stain cell organelles containing nucleic acids for histological purposes. Chemotherapy was in its infancy. Indeed, the discovery of antibiotics, the quantum leap that led to the emergence of chemotherapy as a life-saving modality completely revolutionizing medicine, also threw up the first antibiotic found to be effective in the treatment of cancer (actinomycin D, which is another DNA binder), all prior to the work of Watson and Crick.[3,4] Now more than 50 years after the structure of DNA was published, it is well recognized that controlled regulation of the expression of individual genes by ligands that target and bind to DNA so as to alter its structure and function, has enormous potential for the therapy of genetic diseases as well as the development of diagnostic agents and research tools for functional genomics.[5−7]

Historically, intercalation was the first well-defined molecular model to describe drug binding to DNA. It was originally proposed in an effort to explain the mutagenic action of acridines.[8,9] Aminoacridines such as proflavine were often used as antimicrobial agents with reasonable selective toxicity until largely superseded by the widespread introduction of penicillins.[10] One of the salient features of intercalation is that it separates neighboring base pairs as the drug inserts, leading to helix unwinding of around 11° to 26°.[11,12] Intercalation can interfere with normal DNA functions like transcription and replication through inhibition of polymerases as well as the DNA-unwinding actions of helicases and topoisomerases.[13,14] Because these functions are significantly increased in tumor cells, many intercalating drugs have become common anticancer agents.

A valuable strategy to enhance affinity and specificity for binding to DNA is to make drugs that are multivalent.[15−17] One such, the bis-naphthalimide Elinafide, first identified as a bis-intercalator in 1996,[18] has entered clinical trials after showing exemplary activity against certain human tumors in vitro.[18] Multivalency has been recognized as a common strategy used by nature to increase the overall binding strength of molecular recognition events through taking advantage of entropic gains resulting from prepositioning.[19,20] The nature of the linkage between intercalating groups must define their geometric arrangement and is crucial for efficacy. Originally acridines and other intercalators were linked together via a flexible carbon chain to allow considerable degrees of freedom for the intercalating moieties. These drugs exhibited tighter binding (K_D[a]) than their homologous monofunctional intercalating ring systems,[15,17,21] although the increment from bifunctionality was far from the square that some workers imagined and the need

* To whom correspondence should be addressed. Tel.: int+61883036911 (R.A.R.); int+441223766048 (F.H. and M.J.W.). Fax: int+61883036911 (R.A.R.); int+441223766002 (F.H. and M.J.W.). E-mail: richard.russell@adelaide.edu.au (R.A.R.); fh111@cam.ac.uk (F.H.); mjw11@cam.ac.uk (M.J.W.).

† Equal contribution.

‡ Department of Biochemistry, University of Cambridge, U.K.

§ Department of Pharmacology, University of Cambridge, U.K.

|| Central Queensland University.

⊥ Deakin University.

University of Adelaide.

[a] Abbreviations: DNase, deoxyribonuclease; MOLRAC, molecular rack; K_D, dissociation constant; pBS plasmid, BlueScript plasmid; *tyr*T, gene encoding transfer RNA 1 for tyrosine; K_{app}, apparent binding constant; NMR, nuclear magnetic resonance; MM2, molecular mechanics calculator 2; alternating G−C DNA, poly(dG−dC)·poly(dG−dC); alternating A−T DNA, poly(dA−dT)·poly(dA−dT); G+A, chemical sequencing for guanine and adenine; dsDNA, double-stranded (duplex) DNA; ssRNA, single-stranded RNA; dsRNA, double-stranded RNA; AMV, avian myeloblastosis virus; DMSO, dimethyl sulfoxide; BPES, buffered phosphate EDTA saline; TN, tris-NaCl; TBE, tris-borate-EDTA; ACE reaction, Alkene + Cyclobutene Epoxide reaction; THF, tetrahydrofuran; TBHP, *tert*-butyl hydroperoxide; DCC, *N*,*N*′-dicyclohexylcarbodiimide; TLC, thin layer chromatography; DCM, dichloromethane; TFA, trifluoroacetic acid; DMF, dimethyl formamide: Pet, petroleum.

10.1021/jm0613020 CCC: $37.00
Published on Web 04/13/2007

Scheme 1. Design of Potential Bisintercalators[a]

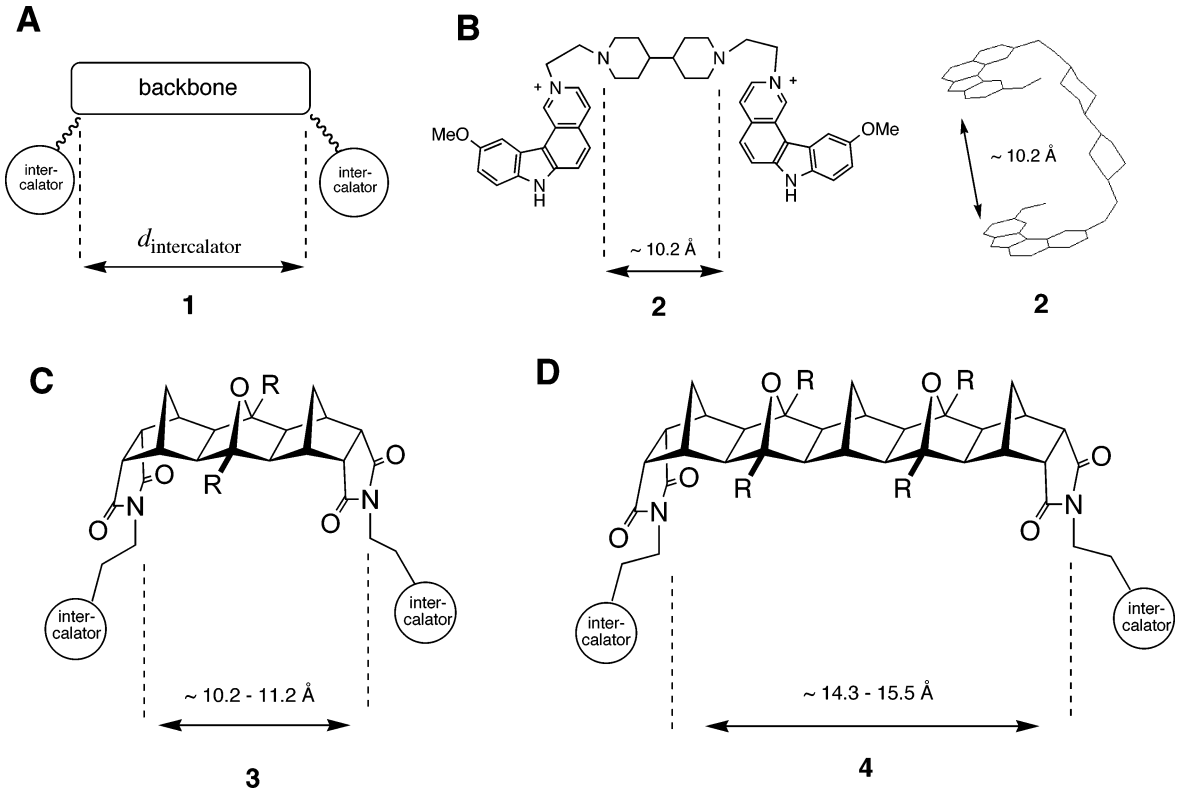

[a] **(A)** The basic design of the potential bisintercalators used in this study: a backbone with two appended intercalating moieties. The distance between intercalator attachment points is an important feature for successful bis-intercalation. (**B**) Structure of ditercalinium **2**, whose two-dimensional projection structure is shown as well as its three-dimensional structure when complexed to DNA;[28,29] the distance between intercalator attachment points is 10.2 Å. Our new compounds have a more rigid backbone, namely, [3]-polynorbornane in **3** and [5]-polynorbornane in **4**. The distances between intercalator attachment points (based on a calculation using mm2)[31] are estimates and vary as indicated depending on the nature of the appended intercalative ring systems.

to use fairly high salt concentrations to suppress self-stacking, and so on, led to relatively weak binding constants for some genuine acridine bis-intercalators.[15,17] With a few exceptions[11] it is generally accepted that bis-intercalation is governed by the nearest neighbor exclusion principle, which stipulates that the intercalating moieties must sandwich a minimum of two base-pairs, demanding a distance between chromophores for bifunctional intercalation of 10.2 Å.[11,22] Simple aminoacridines linked via their N-9 position show an approximately 10-fold increase in binding constant for the bi- versus the monofunctional compounds, with C_6 and C_8 chains bringing about an inter-chromophore separation of the order of 8.8 and 11.3 Å between the N-9 positions of the intercalative rings.[15,17] Although these flexible linkers improve binding through cooperativity, some bis-intercalators have been shown to "creep" along the helix with fast chromophore exchange kinetics rather than remaining bound at one site on the DNA backbone, resulting in low sequence selectivity.[23] By contrast, more rigid linkers tend to favor slower exchange kinetics as well as enhancing antileukaemic activity in vivo.[23] Flexibility and orientational freedom increase the likelihood of entropically favorable bis-intercalation but the sort of precise positioning that brings about well-defined contacts leading to efficient molecular recognition is elusive in these compounds.

Accordingly, we reasoned that the improved molecular recognition attainable by using a rigid linker might prove more favorable for producing sequence-selective bifunctional compounds in the first place. To explore the requirements for rigid positioning of two intercalators potentially endowed with higher sequence selectivity,[24] we synthesized and probed a series of compounds seeking to exploit the principle of multivalency in the special context of DNA intercalation. In the series of potential bis-intercalators that we designed,[25] individual building blocks were joined by BLOCK synthesis to create larger complexes with defined stereochemistry. In these compounds, a varying number of norbornane rings form the backbone (dubbed the molecular rack, "MOLRAC"), attached to which are a pair of planar, aromatic ligands.[26,27]

We have studied in detail the intercalative properties of nine such novel compounds, comparing mono- and bivalent compounds, varying backbone lengths, and employing several pendant intercalating groups. In particular, we have compared binding specificity and DNA helix unwinding, using competition dialysis, unwinding assays, and DNase I footprinting, to derive structure−reactivity relationships. Our tests have identified one sequence-selective bis-intercalating compound, **3a**, with an unwinding angle of 27° and a binding constant of 8 μM.

Results

Design. Prior to our work, structural information on oligonucleotide complexes of ditercalinium **2** (Scheme 1)[28] and triostin A[29,30] suggested an optimal distance between chromophores, $d_{intercalator}$, of 10.2 Å, combined with a slightly bent backbone geometry when bound to DNA. We aimed to mimic the curved framework of these natural products using rigid polynorbornane backbones in our general target structures **3** and **4** (Scheme 1). These simple [3]- and [5]-polynorbornane backbones were substituted with two known intercalators symmetrically attached to the *endo*-positions. Specific target MOLRAC compounds with different chromophores and bridgehead substitutions are shown in Table 1.

Table 1. Summary of DNA Binding Data for Intercalating MOLRAC Compounds[a]

compound	structure	ϕ (°) [b]	intercalation type	K_d (μM) [b]	([intercalator]: [bp])^{complete} [c]
12	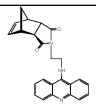	**U**	mono		> 1.5
3a	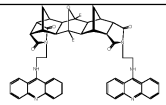	**-26.8 ± 4.4**	bis	8.3 ± 3.1	0.04 ± 0.01
3b	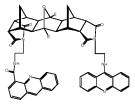	**-12.1 ± 1.1**	mono	21.3 ± 0.3	0.10 ± 0.02
4a	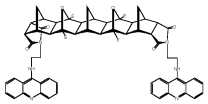	**-11.2 ± 0.5**	mono	10.8 ± 1.5	0.10 ± 0.05
4b	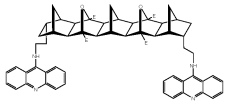	**-15.2 ± 0.7**	mono	1.0 ± 0.7	0.06 ± 0.02
3c	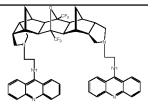	**U**	mono		1.0< x< 1.5
3d	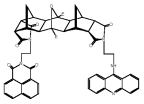	**U**	mono		> 1.5
3e	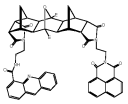	**-**	NO		**-**
3f	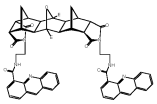	**-**	NO		**-**

[a] Conditions: [Tris-HCl] = 50 mM, pH 7.5, [KCl] = 50 mM , [$MgCl_2$] = 10 mM, [DTT] = 0.5 mM, [EDTA] = 0.1, [BSA] = 200 μg/mL. E = CO_2Me. [**U** = Slight unwinding is observed and mono-intercalation of the ligand presumed. NO = No intercalation was detected in one-dimensional gels. These refer to the one-dimensional gels of Figure 2]. [b] ϕ angles and K_d are determined by two-dimensional assay as in Figures 4 and 5. (**U**: slight unwinding detected at high [intercalator]; NO: no unwinding detected). [c] ([Intercalator]/[bp])^{complete} is the ratio of intercalator molecules per base pair of DNA at which supercoiling appears essentially complete, as read from the one-dimensional gels [see Figure 1].

Simple preliminary MM2 calculations confirmed that the interchromophore distances, $d_{intercalator}$, lie within the required range, namely, between 10.2 and 11.2 Å for **3** and 14.3−15.5 Å for **4**, the exact value depending on the substitution pattern on the backbone.[31] While the structure of the rigid backbone framework and the separation of the intercalator attachment points $d_{intercalator}$ can be modeled with reasonable accuracy, any flexibility in the side chain will permit a variety of conformations where the intercalators are separated by different distances. The optimal conformation will depend on the energetics of the interaction with DNA and cannot easily be predicted. This was addressed in biological assays.

Synthetic Strategy. Functionalized [*n*]-polynorbornanes such as **3** and **4** are versatile molecular frameworks that provide a geometrically adjustable backbone to support biologically active moieties.[32] In particular, the length and curvature of [*n*]-polynorbornanes **1** and their heterocyclic analogues can be adjusted by judicious choice of building BLOCKs.[26,27,33]

Two general strategies, both variations of the BLOCK approach,[34] were employed to accomplish the synthesis of the desired target molecules. The first of these (Scheme 2A) shows the "gluing reaction" in which two identical norbornenes **5** are joined via a sequence of cyclo- and retrocycloadditions with substituted oxadiazole **6**. Scheme 2B shows the ACE reaction,[34] which joins two BLOCKs, namely, a norbornene **5** and an electron-deficient epoxide **7**. This latter process involves the 1,3-dipolar cycloaddition of a carbonyl ylide generated by the thermal ring opening of an electron deficient epoxide to a norbornene. These reactions are tolerant toward a wide range of functionality on the reactants.[26,34,35]

Synthesis of [3]-Polynorbornanes. The desired [3]-polynorbornanes, **3a**, **3b**, and **3d**−**f** (but not **3c**), share a common framework that is readily accessible via the ACE reaction. Thus, the bis 9-aminoacridine derivative **3a** was prepared from two BLOCKs (**12** and **14**) as outlined in Scheme 3.

Scheme 2. Key Reactions Used in the BLOCK Approach to the Synthesis of [3]-Polynorbornanes of Structural Type 3[a]

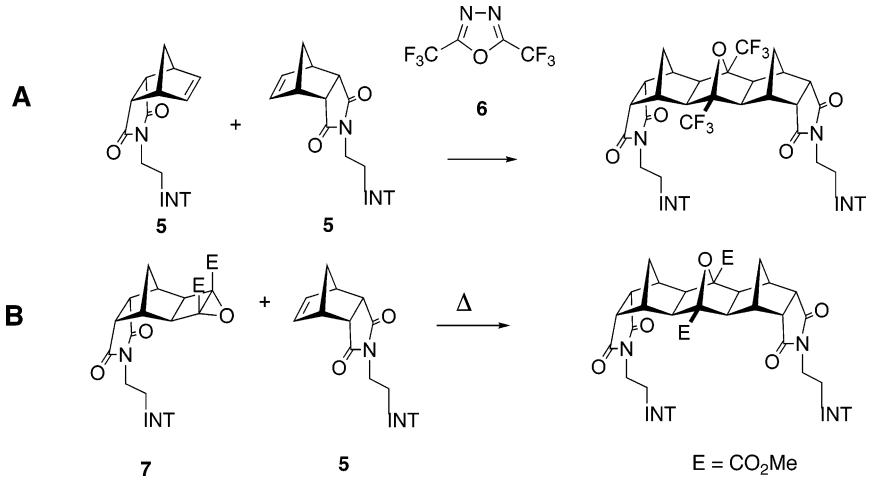

[a] (**A**) The "gluing reaction" connects two norbornane BLOCKS **5** using the oxadiazole **6**. (**B**) The ACE reaction in which a cyclobutene epoxide **7** reacts with a norbornene **5**.

Scheme 3

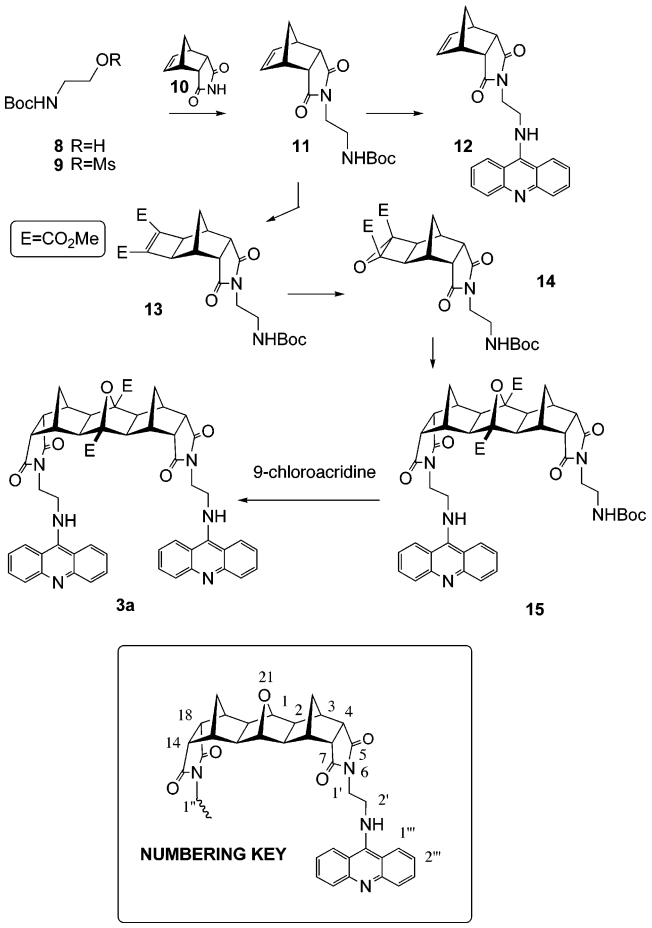

Central to this synthesis was the construction of imide **11**, which was readily prepared in two steps from the cycloadduct **10** of cylopentadiene and maleimide and the protected ethanolamine **9**. Mild deprotection of the alkylated imide **11** with trifluoroacetic acid in dichloromethane afforded **22** in excellent yield. This compound could be condensed with 9-chloroacridine to afford the desired product (**12**) in 68% yield. The intermediate **11** also served as the starting point for the other half of the target molecule, **3a**. Thus, a straightforward Ru^0-catalyzed [2+2] cycloaddition with dimethyl acetylene dicarboxylate[36,37] afforded the cyclobutene **13**, which was subjected to epoxidation with potassium *t*-butoxide and *t*-butyl hydroperoxide[32] to afford **14**. The stereochemistry of this combination of reactions is well documented,[26,34,35] and spectroscopic measurements were entirely consistent with the proposed structures.

Reduction of the imide **10** with lithium aluminum hydride proceeded smoothly to afford the corresponding cyclic amine **16**, which was subjected to a "gluing" sequence[38,39] of reactions with 2,4-bis(trifluoromethyl)oxadiazole, followed by alkylation with the ethanolamine derivative **9**. Reaction of the diamine **17** with 9-chloroacridine furnished the symmetrical compound **3c** (Scheme 4).

The synthesis of the mixed [3]-polynorbornane **3b** (Scheme 5) required the preparation of the amide **22**, derived from acridine-4-carboxylic acid. This was achieved in two steps from epoxide **14**. As observed previously,[40] electron-deficient epoxides exhibit remarkable stability in both acid and base and accordingly tolerate a wide variety of reaction conditions. Thus, the Boc group was smoothly removed with trifluoroacetic acid in dichloromethane, over a period of 14 h, and the resulting amine **19** was coupled with acridine-4-carboxylic acid in the presence of DCC. BLOCK **20** was subsequently condensed with the acridine derivative **12** (Scheme 3) to yield the mixed structure **3b**.

Having successfully prepared the epoxide derivative **20**, similar chemistry was used to convert the maleimide derivative **21** into the acridine **22**. Coupling of compounds **20** and **22** afforded the symmetrical [3]-polynorbornane **3f** in a modest yield of 43% (Scheme 6).

Access to the desired structures **3d** and **3e** containing a naphthalimide moiety was achieved from the key intermediate epoxide **27**. Although we were able to establish a number of routes to **27**, this molecule was best prepared as shown in Scheme 7 by a strategy that left the introduction of the epoxide until the final step. Condensation of epoxide **27** with the previously prepared BLOCKS **12** and **22** afforded the [3]-polynorbornanes **3d** and **3e**, respectively.

Synthesis of [5]-Polynorbornanes. The [5]-polynorbornanes **4a**−**c** were synthesized by means of a double ACE reaction centered around the bis-epoxide **28** (Scheme 8), which was prepared as previously described.[26,34,35] Reaction of one equivalent of bis-epoxide **28** with two equivalents of the acridine **12** afforded the symmetrical bis-imide derivative **4a**.

The remaining [5]-polynorbornane target molecule was less straightforward, as it contains two chiral centers, one at each

Scheme 4

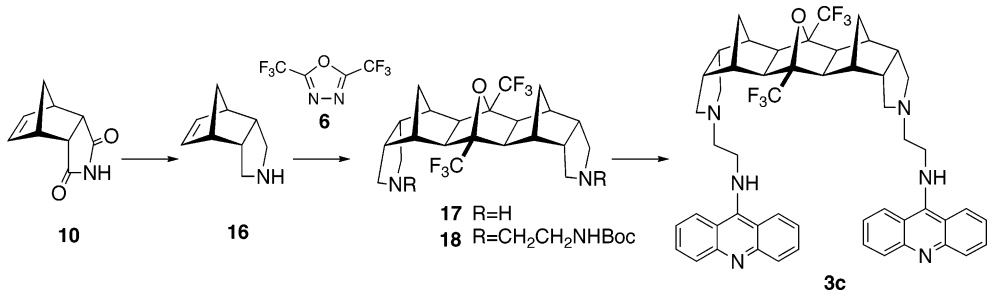

Scheme 5

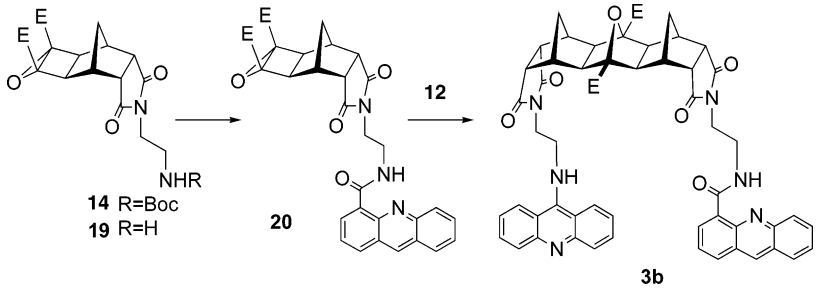

Scheme 6

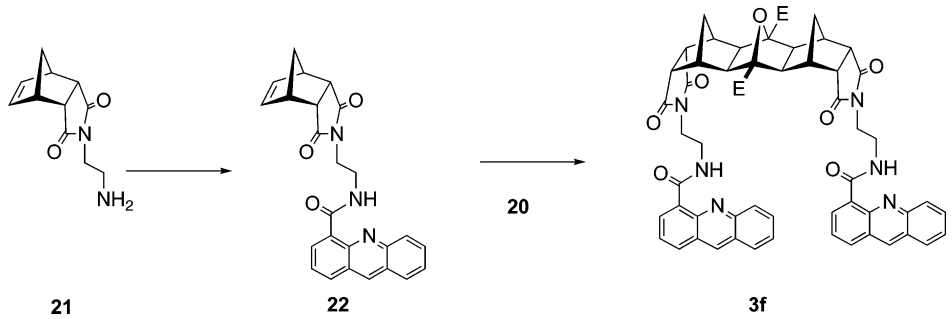

Scheme 7

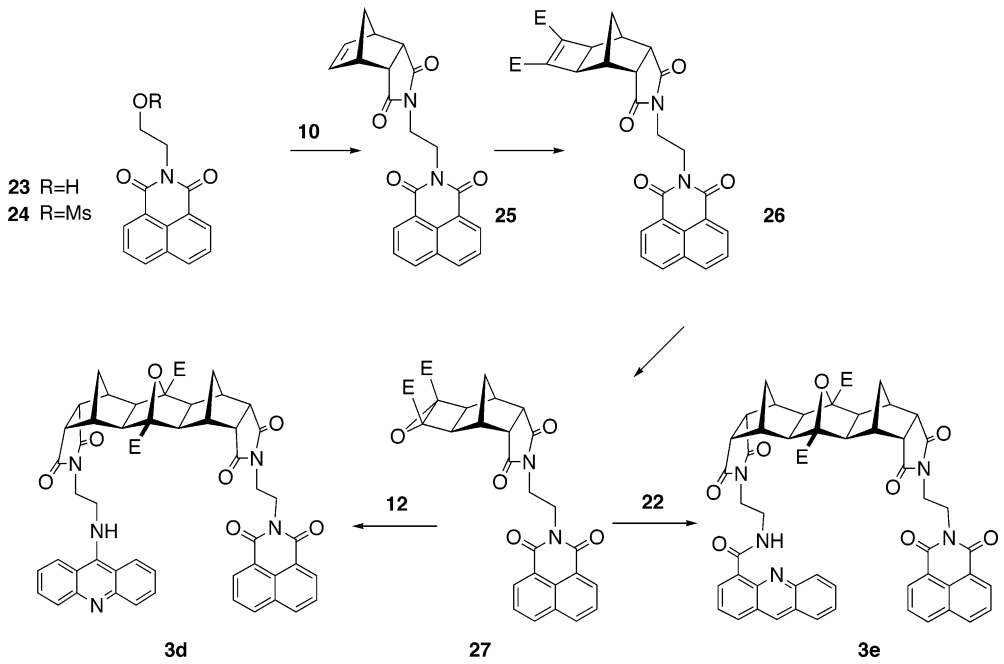

end of the molecule. While we have subsequently developed syntheses of all of the individual stereoisomers, the material used in this study comprised a racemic mixture of the chiral product **4b** and the *meso* compound **4c** (hereinafter referred to as **4b**/**c**; Scheme 9). Thus a Diels Alder reaction of cyclopentadiene and acrylonitrile afforded the known adduct **29**,[41] which was subsequently reduced with lithium aluminum hydride to furnish the corresponding primary amine. Condensation of this

Scheme 8

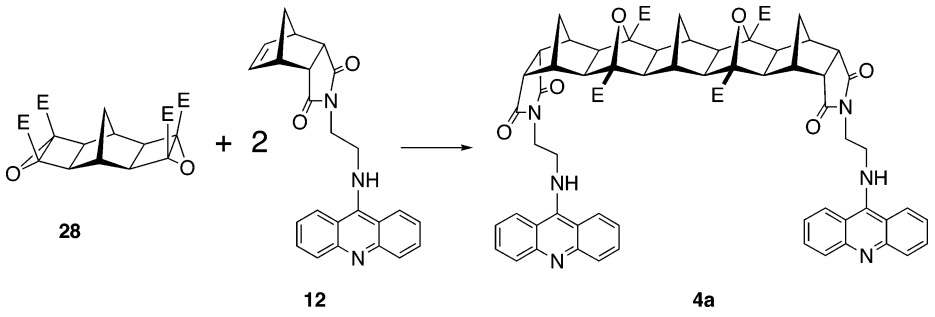

Scheme 9

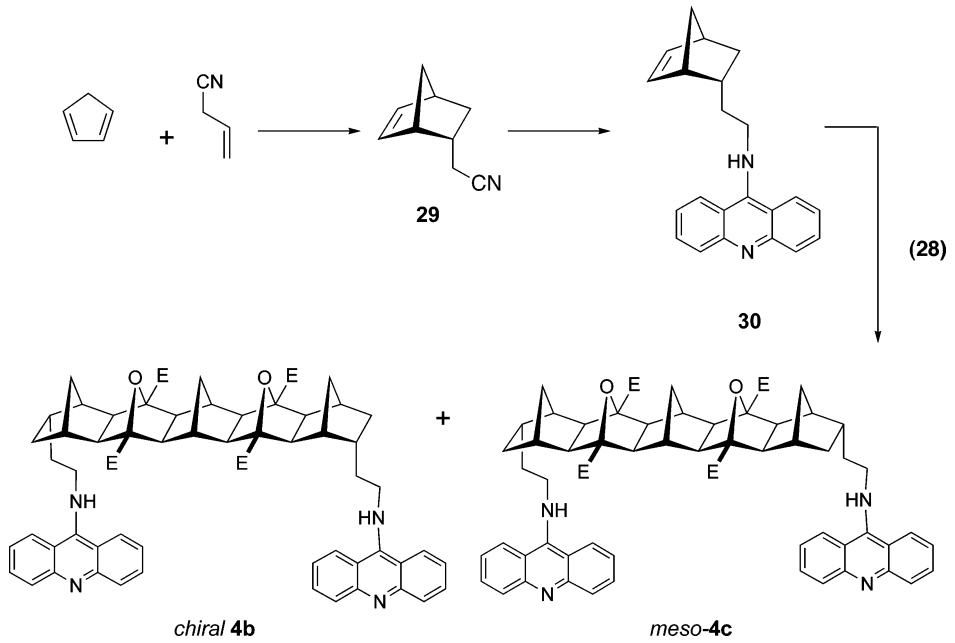

amine and the rather unstable product with 9-chloroacridine in DMSO gave the racemate **32** in 78% yield. Subsequent reaction of this latter compound with bis-epoxide **28** yielded the mixture of **4b**/**c**.

Competition Dialysis. A competition dialysis screen was used to determine the relative binding of the MOLRAC compounds to eight different polynucleotides. This assay affords a simple, unambiguous method to compare polynucleotide-binding properties of multiple compounds.[42−44] The data were used to calculate mean apparent binding constants recorded in Table 2. The mean error was around 10%, consistent with previous studies.[45] One compound, **3e**, was insufficiently soluble for the assay, probably because of its high content of hydrophobic constituents.

The eight assayed compounds exhibited greatest affinity for the duplex DNA species and bound less well to single-stranded polynucleotides, a result commonly encountered with intercalators as well as other DNA-binding compounds.[46] Bifunctional MOLRAC compounds were found to display generally higher affinity for duplex DNA than the monofunctional compound **12**, and in several cases (**4a**, **3b**, **3a**, and **3c**), the average affinity was more than double that of **12**, illustrating an intrinsic advantage of bifunctionality. It was also apparent for all but one of the eight compounds that the preferred polynucleotide species was poly(dA−dT)•poly(dA−dT) [alternating poly A−T DNA], suggesting a notable binding preference for AT-rich sequences. Interestingly, this was especially pronounced for the monofunctional compound **12**. Given this observation, comparison of affinity toward this duplex polynucleotide provides an immediate indication of structure−activity relationships among the ligands. For example, a scaffold comprising three polynorbornane rings appears to be marginally preferred to five rings (20% decrease in affinity). Furthermore, when comparing functional intercalating groups, two aminoacridines emerge quite clearly as the preferred polycyclic ring systems; substitution of either one with acridine-4-carboxamide or especially naphthalimide results in loss of binding affinity (24 and 63% decreases, respectively).

Electrophoretic Assay for Binding and Intercalative Unwinding. To further investigate structure−activity relationships, DNA helix-unwinding and binding characteristics were examined by relaxing closed circular duplex DNA in the presence of the experimental ligands. In the first series of tests, MOLRAC compounds were incubated with supercoiled circular DNA (pUC19) at a range of concentrations (and thus, at varying ratios of intercalator to base pairs), relaxed with topoisomerase I, and the products were resolved by one-dimensional agarose gel electrophoresis. A set of sample images is shown in Figure 1. Topoisomerase I relaxes the negative supercoiling of circular DNA, but the change in linking number is smaller if a helix-unwinding ligand is bound; this leads to the reappearance of supercoiled topoisomers when molecules "relaxed" in the presence of ligand are subsequently electrophoresed in the absence of the ligand.[47] Doing the test over a range of concentrations eliminates the possibility that the ligand merely inhibits the activity of topoisomerases I. A straightforward one-

Table 2. Apparent Binding Constants (K_{app}) of MOLRAC Compounds for Eight Polynucleotide Species, as Determined by Competition Dialysis[a]

		mean apparent binding constant: K_{app} 10^3 (M^{-1})								
compound		**12**	**3a**	**3b**	**3c**	**3d**	**3e**	**3f**	**4a**	**4b/c**
functional groups		AA	AA-AA	AC-AA	AA-AA	NI-AA	NI-AC	AC-AC	AA-AA	AA-AA
scaffold length		1	3	3	3	3	3	3	5	5
adapter		2C CI	2C CI	2C CI	2C EP	2C CI	2C CI	2C CI	2C CI	2C mix
polynucleotide										
E. coli DNA	dsDNA	3.47	32.80	12.93	19.07	14.93	NS	6.80	25.73	14.40
Calf thymus DNA	dsDNA	6.27	30.40	23.07	20.27	8.13	NS	16.00	30.40	13.73
poly(dAdT)· poly(dAdT)	dsDNA	12.13	38.93	29.47	29.47	14.40	NS	13.87	31.73	10.53
poly(dGdC)· poly(dGdC)	dsDNA	3.47	28.40	15.60	27.60	8.13	NS	9.60	26.40	13.07
poly(dA)· poly(dT)	dsDNA	0.53	16.40	0.80	19.60	3.87	NS	6.80	23.73	8.67
polyA·polyU	dsRNA	1.47	19.20	0.27	0.53	0.80	NS	8.27	25.47	6.00
wheat germ RNA	ssRNA*	2.40	8.80	0.27	0.53	7.60	NS	0.53	5.33	5.33
polyA	ssRNA	0.00	2.93	0.27	1.73	0.80	NS	0.53	1.47	6.00

[a] Conditions: 6 mM Na_2HPO_4, 2 mM NaH_2PO_4, 1 mM EDTA, 185 mM NaCl, pH 7.1; 1 μM MOLRAC compound, 75 μM polynucleotide; dialysis across 7000 MWCO membrane for 24 h. AA = aminoacridine, AC = acridine-4-carboxamide, NI = naphthalimide, CI = cyclic imide, EP = *endo*-pyrrolidine, 2C = 2-carbon alkyl, mix = racemic compounds, NS = not sufficiently soluble to be tested, ssRNA* = some dsRNA also expected to be present.

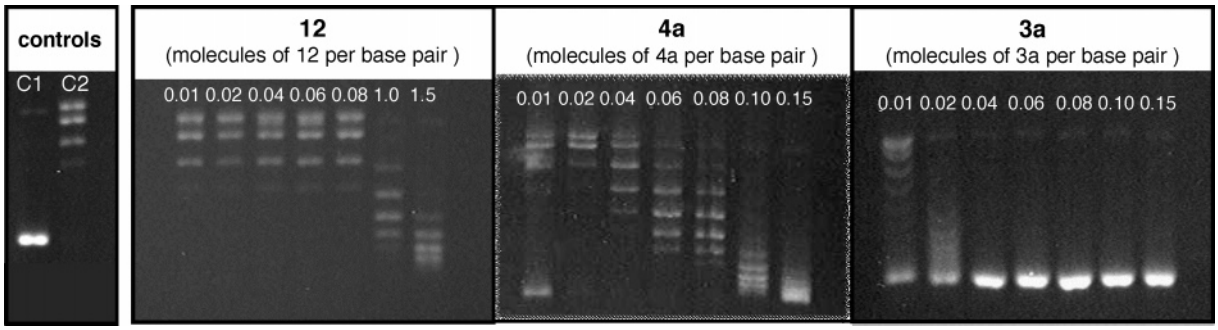

Figure 1. Comparison of mono and divalent intercalators **12**, **4a**, and **3a** in a one-dimensional unwinding assay. Compound **3a** drives ccDNA to full supercoiling at an [intercalator]/[bp] between 0.02 and 0.04, and **4a** achieves the same effect at more than double the amount of ligand (~0.1), whereas **12** requires a ratio of >1.5. Each compound was incubated with closed circular duplex DNA at varying ratios of intercalator to base pairs and relaxed by topoisomerase I (37 °C, 4 h). Conditions: 50 mM Tris-HCl pH 7.5, 50 mM KCl, 10 mM $MgCl_2$ 0.5 mM dithiothreitol, 0.1 mM EDTA, 200 μg/mL bovine serum albumin. Controls: C1, no topoisomerase; C2, no intercalator.

dimensional gel detecting the presence of topoisomers can, therefore, be employed to reveal DNA intercalation. From this assay we can establish a characteristic ratio, $([\text{intercalator}]/[\text{bp}])^{\text{complete}}$, at which the reappearance of supercoiling appears essentially complete (Figure 1). This ratio is admittedly a composite measure of binding strength (K_D) as well as the unwinding angle ϕ, but it has proved useful in screening homologous series of drugs.[48,49]

By this means, we first compared a molecule that proffers only one 9-aminoacridine substituent for intercalation (**12**) with bifunctional molecules that have two 9-aminoacridine arms. The monovalent compound has the highest $([\text{intercalator}]/[\text{bp}])^{\text{complete}}$. Figure 1 displays data for **12** side-by-side with bivalent **3a**. Full supercoiling is reached much earlier for **3a**, between 0.02 and 0.04 molecules of **3a** per bp, while full reappearance of supercoiling is not observed even at the highest accessible ratio of 1.5 molecules of **12** per bp. Monovalent **12** is thus a weak intercalator, because a 40-fold higher concentration is needed to produce the same effect as its bifunctional homologue **3a**. When **3a** with three norbornane systems was compared to **4a** with five norbornane systems, the ratio $([\text{intercalator}]/[\text{bp}])^{\text{complete}}$ increased from 0.04 to over 0.1 (Figure 1). Changing the anchoring attachment to shorten the backbone by removing two maleimide moieties, for example when **4a** is compared to **4b**/**c**, leads to almost a halving of $([\text{intercalator}]/[\text{bp}])^{\text{complete}}$ down to 0.06 (Table 1). Intercalating substituents other than 9-aminoacridine, as in **3d**, **3e**, and **3f**, sharply reduce the ability to bind and intercalate (Table 1).

Following the qualitative insights provided by one-dimensional gel electrophoresis, selected compounds were further analyzed quantitatively using a two-dimensional gel procedure introduced by Zeman and Crothers.[47,50] Serially diluted topoisomerase I relaxation reactions at a constant [intercalator]/[DNA] ratio were performed, and the resulting apparent unwinding of the closed circular DNA was used to calculate unwinding angles and intrinsic dissociation constants (K_d). This is illustrated in Figure 2 for the MOLRAC compound **3a**, where the "raw data" images are shown. The subsequent mathematical analysis after densitometric scanning of the gel is explained in Figure 3. Results for the four compounds that produced significant unwinding are compared in Figure 4, and the complete findings from both the one- and two-dimensional gel electrophoresis assays are recorded in Table 1.

The compiled results indicate the affinity of each compound for DNA (K_D) and also describe the intercalation type, as determined by the helix-unwinding angle. Where full analysis by the laborious two-dimensional gel procedure was not possible, the ratio $([\text{intercalator}]/[\text{bp}])^{\text{complete}}$ still gives a useful indication, as it is a composite measure of binding strength and unwinding angle. Two compounds (**3e** and **3f**) were found to have no detectable effect on topoisomerase I relaxation at all, and three further compounds (**12**, **3d**, and **3c**) were found to have only mild unwinding properties. With the exception of **3c**, all of these compounds also displayed conspicuously low affinity for binding to duplex DNA in the competition dialysis assay. Of the compounds that unwound DNA sufficiently to

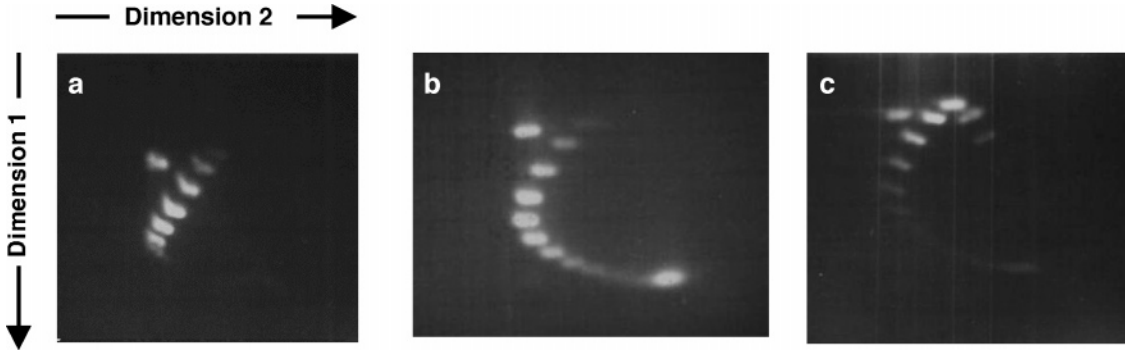

Figure 2. Resolution of topoisomers by linking number on two-dimensional gels. pUC19 circular DNA was relaxed by topoisomerase I in the presence of various concentrations of **3a**. The first dimension separates topoisomers with different ΔLk; the second dimension separates topoisomers of identical *absolute* linking number |ΔLk|, with positive linking numbers running faster than negative ones. Panels (a), (b), and (c) show two-dimensional gels of pUC19 DNA incubated with **3a** at a constant ratio of DNA base pairs to molecules of **3a**, namely, 36.6 bp/molecule of intercalator, but different dilutions. Conditions: 1% agarose gel; 50 mM Tris-HCl pH 7.5, 50 mM KCl, 10 mM $MgCl_2$ 0.5 mM dithiothreitol, 0.1 mM EDTA, 200 μg/mL bovine serum albumin. Panel (a): [**3a**] = 3.5 μM; total volume 47 μL. Panel (b): [**3a**] = 1.9 μM; total volume 87 μL. Panel (c): [**3a**] = 1.0 μM; total volume 167 μL.

permit full two-dimensional gel analysis, **3a** was set apart as the only compound that unwound DNA by an angle that clearly indicated bis-intercalation, namely, −27° (Figure 3). The other three compounds only unwound DNA about half as much, consistent with binding restricted to mono-intercalation, suggesting that only a scaffold length of three polynorbornane rings is capable of forming a bis-intercalator. The affinity of **3a** for DNA as given by K_D is actually comparable to that of **4a** and between two and three times that of **3b**. However, dissociation constants do not necessarily relate simply to bivalent versus monovalent binding. Interestingly, it was found that **4b**/**c** seemed to have the highest affinity for DNA, with a dissociation constant some 10-fold lower than was found for **4a**. This unexpectedly tight binding of **4b**/**c** represents the only apparent inconsistency between DNA affinity measurements derived from the unwinding and competition dialysis assays.

DNase I Footprinting. The MOLRAC compounds found to have the highest affinity (**4b**/**c**) and largest unwinding angle (**3a**) were examined by DNase I footprinting, along with the monomeric **12**. Footprinting is the method of choice for analyzing sequence-selective DNA-binding properties and can be used to provide measurements of binding affinity as well as sequence-selectivity.[51−53] Initially, the three compounds were titrated against a standard 265 bp DNA fragment from pBS plasmid DNA; however, neither **12** or **4b**/**c** were found to alter the DNase I pattern other than by globally decreasing cleavage throughout the DNA sequence (Supporting Information Figure S1). By contrast, the introduction of **3a** led to sequence-specific decreases (and increases) in DNase I cleavage (Figure 5A). This was confirmed by exposing **3a** to a different DNA fragment containing the well-investigated *tyr*T promoter (Figure 5B). Both gel images were quantitatively analyzed by densitometry according to an established protocol[54] to yield differential cleavage plots that graphically illustrate the sequence-specific interaction of the compound with DNA (Figure 6).

In agreement with the competition dialysis and unwinding assays, the footprinting experiments showed compound **3a** to bind to DNA with the same affinity as compound **4b**/**c** (global decreases in cleavage seen at 8 and 10 μM, respectively). However, under the scrutiny of the more accurate densitometric analysis, it was apparent that on both pBS and *tyr*T DNA, **3a** generated footprints at specific sequences at even lower concentration, with noticeable binding as low as 1 μM. Across both sequences analyzed, nine sites of footprinting were observed (Table 3), giving an occurrence rate of approximately one site per 16 bp, a frequency lower than that expected for the random occurrence of a single dinucleotide. The sites range in size from 3 to 10 bp, probably reflecting multiple close sites in several instances, especially in *tyr*T DNA. The threshold concentration required to produce an observable decrease in cleavage at the different sites varies, suggesting a degree of selectivity considerably more demanding than simply a requirement for one particular dinucleotide. For example, the *tyr*T DNA site at nucleotide 90 (Table 3, site 9) shows footprinting at a concentration as low as 1 μM compared to 4 μM for the site at nucleotide 70 (Table 3, site 8). Taken together, these findings help to characterize **3a** as a compound that binds in a bis-intercalating fashion with some selectivity for DNA sites containing three or more base pairs. The obvious occurrence of large enhancements of nuclease cleavage flanking the footprinted sites is typically indicative of neighboring intercalation.[55] However, the exact constitution of preferred binding sites for **3a** is not so easy to pinpoint. In Figure 6A (pBS DNA), the five identifiable sites lie near sequences TAG, CTG, ATG, and AGT, suggesting that perhaps the TpG dinucleotide (and/or its complement CpA) is a common component of preferred sites. However, in *tyr*T DNA, the same motif is hard to perceive, though it is noteworthy that the ostensibly tightest site noted above, round position 90 (Table 3, site 9), does contain the TpG motif and actually forms part of the so-called TATA box for this promoter. This sort of sequence preference pattern has been noticed before with other drugs and might reflect little more than the relative ease of unstacking certain sequences, doubtless a prerequisite for intercalation.[18,54]

Discussion

Four assays have been employed to investigate the molecular recognition properties of MOLRAC compounds. Both competition dialysis and one-dimensional gel electrophoresis yielded a rudimentary measure of DNA binding, allowing a ranking of the compounds in terms of activity. However, to secure a more thorough understanding of the molecular recognition as well as structure−activity relationships for the lead compounds, it was necessary to select a few examples for examination by the Zeman−Crothers treatment as well as DNase I footprinting experiments.

The series was devised around three types of intercalative polyaromatic ring systems attached in a variety of ways to polynorbonane linker scaffolds of increasing length. Judged by all the methods of assessment, the compounds with the highest affinity toward duplex DNA species were those that contained

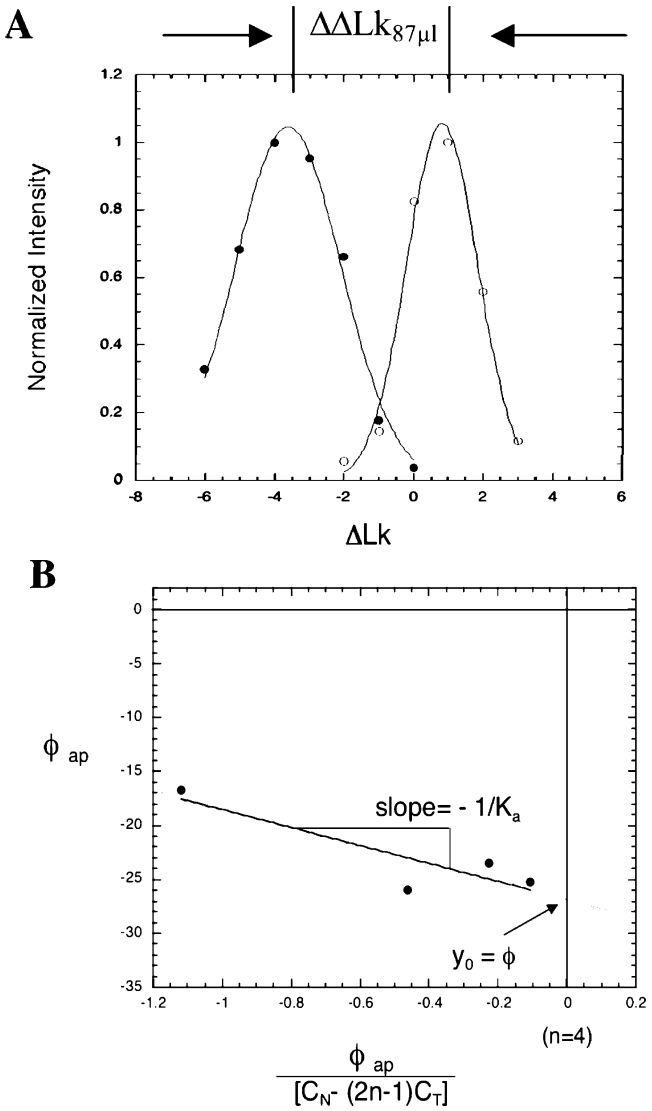

Figure 3. Determination of unwinding angle and K_D for **3a** from two-dimensional gels. (**A**) Boltzmann distributions of topoisomers corresponding to gel (b) of Figure 2 (open circles) and of a control run without **3a** (closed circles), fitted to $I = I_M \exp[-w(\Delta Lk_c - \Delta Lk_c^0)]$; I = integrated band intensity; I_M = maximum band intensity at the peak of the topoisomer distribution; w = width of the distribution. $\Delta\Delta Lk$ is determined for each reaction and used to calculate one point of the binding isotherm. (**B**) Zeman−Crothers plot in which the apparent unwinding angle (ϕ_{ap}) is plotted on the ordinate against $\phi_{ap}/[C_N - (2n - 1)C_T]$ on the abscissa. $\phi_{ap} = 360\ (N_D/N_L)\Delta\Delta Lk_c$. The data are fitted to a linear equation where the ordinate intercept = ϕ (unwinding angle of the intercalator) and the slope = $[-K_a]^{-1}$. N_D = [DNA molecules]; N_L = [ligand or intercalator]; C_N = [bp]; C_T = $[\text{ligand}]_{Total}$; K_a = association constant; n = neighbor exclusion parameter or the number of sites (bp) covered by one molecule of bound ligand. For **3a**, ϕ is $-26.8° \pm 4.4$ and the slope is $-9.16\ \mu M \pm 1.45$. Assuming that **3a** bis-intercalates and obeys the neighbor exclusion principle, the number of base pairs covered by one molecule of bis-intercalator would be $n = 4$.

only 9-aminoacridine moieties. Composites containing acridine-4-carboxamide or naphthalimide chromophores were substantially less effective. Wherever the estimated K_{app} or K_d values of compounds containing the latter groups could be compared to equivalent molecules containing solely 9-aminoacridine moieties, it was clear that they did not benefit DNA binding to any significant extent (cf. Tables 1 and 2). Moreover, compounds containing acridine-4-carboxamide or naphthalimide chromophores were also found to be much less soluble in aqueous solution than MOLRACS constituted with 9-aminoacridine, probably because of protonation of the latter's acridine ring nitrogen. NMR studies of acridine-4-carboxamide have

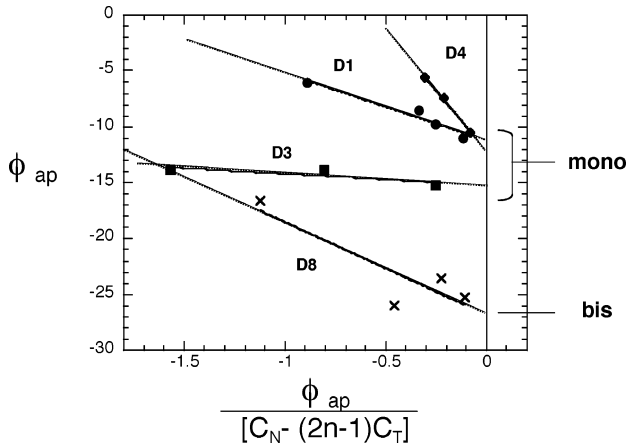

Figure 4. Zeman−Crothers plots comparing the binding isotherms for **4a**, **4b**/**c**, **3b**, and **3a**. Each point is obtained from a two-dimensional gel as described in Figure 3. The unwinding angles (ϕ) and K_Ds for **3b** (◆), **4a** (●), **4b**/**c** (■), and **3a** (×) are summarized in Table 2. Compound **3a** has an unwinding angle double that of **4a**, **4b**/**c**, and **3b**, but **4b**/**c** has the strongest affinity constant of all four compounds. The normalized apparent unwinding angle $\phi_{ap}/[C_N - (2n - 1)C_T]$ was calculated with $n = 2$ for **4a**, **4b**, and **3b**, as they seem to mono-intercalate, and therefore, one molecule would only take up one site, or two base pairs, whereas $n = 4$ was used in the case of **3a**, as explained in Figure 3.

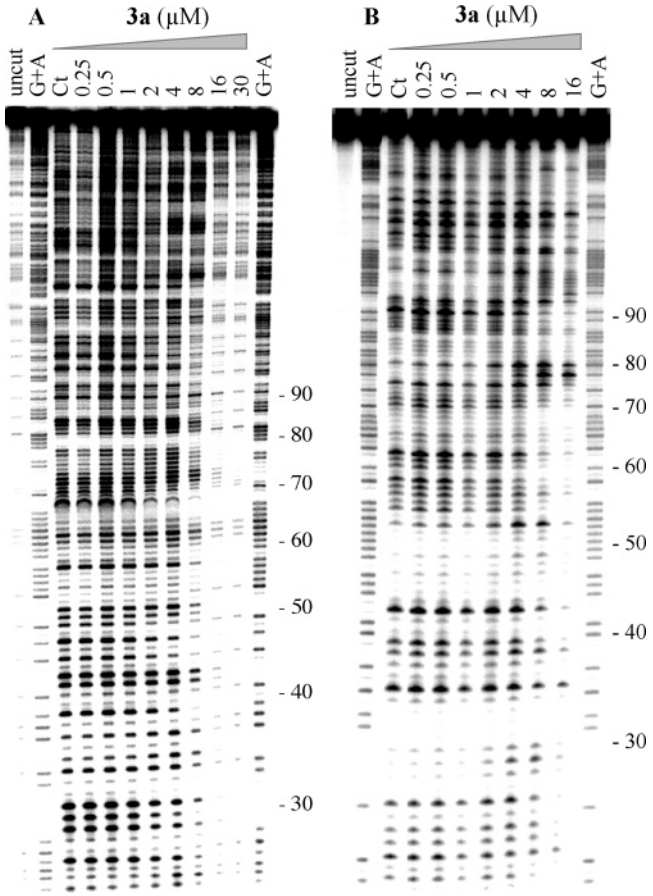

Figure 5. DNase I footprinting of compound **3a** on a 265 bp fragment excised from pBS (A) and a short region encompassing the *tyr*T promoter of *E. coli* (B). Sequence positions are numbered vertically using the chemical sequencing marker lanes (G+A) as a guide. Conditions: 10 mM Tris, pH 7.4, 10 mM NaCl; overnight incubation at room temperature; 8% denaturing polyacrylamide gel.

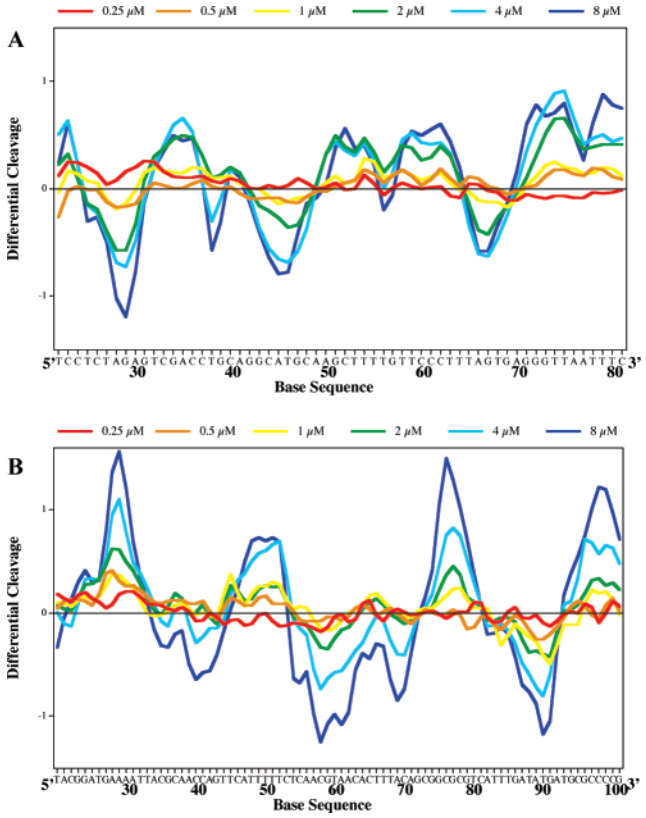

Figure 6. Quantitative analysis of DNase I footprinting results for compound **3a**. Gel images (Figure 5) were analyzed using image quantification software to produce differential cleavage plots for both the 256 bp pBS DNA target (A) and *tyr*T promoter DNA target (B). The ordinate is plotted on a natural log scale, with colored curves corresponding to successively doubling ligand concentrations, as indicated. Negative values (troughs) indicate regions of footprinting.

Table 3. Details of Observed DNase I Footprints Produced by Compound **3a**

	DNA fragment	footprint sequence[a]	nucleotide position	minimum concentration[b]
1	pBS 265mer	5′-tcTAGag-3′ 3′-agATCtc-5′	27−30	2 μM
2	pBS 265mer	5′-CTG-3′ 3′-GAC-5′	35−39	4 μM
3	pBS 265mer	5′-cATGca-3′ 3′-gTACgt-5′	44−47	2 μM
4	pBS 265mer	5′-tAGTga-3′ 3′-aTCAct-5′	65−69	2 μM
5	*tyr*T promoter	5′-aCGC-3′ 3′-tGCG-5′	34−37	8 μM
6	*tyr*T promoter	5′-aCCAgt-3′ 3′-tGGTca-5′	40−43	8 μM
7	*tyr*T promoter	5′-tcaACGtaaca-3′ 3′-agtTGCattgt-5′	57−60	2 μM
8	*tyr*T promoter	5′-tACA-3′ 3′-aTGT-5′	68−71	4 μM
9	*tyr*T promoter	5′-gatATGa-3′ 3′-ctaTACt-5′	88−91	1 μM

[a] Core nucleotide triplet of footprint is shown in uppercase with the flanking footprinted sequence shown in lowercase. [b] The minimum concentration at which densitometrically analyzed band intensities at the footprint site indicate a decrease in DNase I cleavage greater than any associated with noise elsewhere on the sequence.

revealed that it can form an unfavorable, strong intramolecular hydrogen bond to produce an additional six-membered ring.[56] One likely consequence of this property is to reduce the solubility of the chromophore by reducing the number of groups available to form external hydrogen bonds as well as increasing the size and hydrophobicity of the planar ring system.

The clear argument for inclusion of 9-aminoacridine was not mirrored by any obvious benefit conferred by either of the adaptors that were used to attach the intercalative groups to the scaffold. The competition dialysis data (Table 2) suggested that the cyclic imide with a 2-carbon alkyl connection was preferred over the endo-pyrrolidine with a 2-carbon alkyl connection (**3a** vs **3c**). However, just the simple 2-carbon connection of **4b**/**c** on its own appeared to endow relatively strong DNA binding, a finding confirmed by the Zeman−Crothers analysis, where the two-carbon connection of **4b**/**c** was found to confer the highest affinity for DNA, albeit via a mono-intercalating action (Figure 4 and Table 2). To complicate things further, the DNase I footprinting data indicated clearly that the cyclic imide was a major feature contributing to binding affinity. It seems most likely that differences between the assays are responsible for picking up different properties conferred by the various adaptors. The simple two-carbon connection imparts much greater flexibility, allowing more potential interactions with DNA; however, the lack of a defined rigid structure appears to prevent the compound from exhibiting any definite selectivity. This is similar to the reported observations with a six-carbon diacridine, a compound consisting only of two aminoacridines linked by an unbranched *n*-hexyl chain; this compound has a high affinity for DNA but no selectivity due to an over-flexibility that allows it to "creep" along the polymer.[23] Consequently, it appears that the degree of rigidity imposed by the cyclic imide adaptor, as well as potential interactions between the adaptor and the DNA, contribute to bis-intercalation and selectivity in exchange for some decrease in affinity. This conclusion is supported by preliminary competition dialysis and footprinting experiments with the fully purified compound **4b** that has *trans* chiral placement of the adaptors, an orientation that allows the compound to spiral with the helix of the DNA. While this compound binds to DNA better than **3a** (and with double the affinity of **4b**/**c**, its racemic counterpart), it does not footprint on DNA with any measurable selectivity (results not shown).

Along with the preference for 9-aminoacridine moieties attached via rigid adaptors, our results also reveal that the scaffold length is a crucial factor determining whether a MOLRAC compound is capable of bis-intercalation. Initially, we assumed that if any dimerized version of a compound displayed less than double the affinity for DNA of its monomeric counterpart then bis-intercalative binding would be unlikely. On this basis, the competition dialysis and one-dimensional gel analyses pointed to both **4a** and **3a**, with 5- and 3-ring scaffolds, respectively, as the only compounds with the potential to bis-intercalate into DNA. Closer inspection through the use of the Zeman−Crothers analysis revealed, however, that **3a** was the only compound capable of unwinding the double helix sufficiently (−27°) to be characterized as a bis-intercalator.[11] Mono-intercalation by comparable acridine-polyamide conjugates has been reported to yield an unwinding angle of −14 to −15°.[57]

Therefore, the length of the polynorbornane scaffold (and thus the accessible distance between the intercalating groups) was identified as another key determinant of the ability to bis-intercalate. The crystal structures of both triostin A−DNA and ditercalinium−DNA complexes had shown an approximately 10.2 Å separation between intercalating groups.[28,30] For **3a**, it was calculated that the three-ring polynorbornane structure was approximately 10.3 Å in length, whereas the five-ring structure of **4a** was 14.4 Å long (values determined with steric interaction energy minimized by MM2). This leads to an average separation between intercalating groups of 11.2 Å for **3a** and 15.5 Å for **4a**, with some added flexibility due to the two-carbon alkyl

adapters. The conclusion is, therefore, that too great a distance for bis-intercalation separates the chromophores when a five-ring (or longer) polynorbornane scaffold is used, as with **4a**, presumably because it exceeds what can be accommodated by the DNA helical twist. Binding with quite high affinity is still observed for such compounds, however, because one aminoacridine can intercalate, while the scaffold and the other chromophore can probably interact favorably with the floor of the minor groove and/or the sugar−phosphate backbone. Although compounds **3a** and **3c** share similar [3]-norbornane scaffolds and identical intercalating moieties, the presence of trifluoromethyl groups (instead of methyl esters) on the backbone and the loss of imide carbonyl groups on the five-membered linker rings decreases the DNA-binding affinity and diminishes the unwinding efficacy at least 10-fold in the one-dimensional gel assay.

The design principle that gave rise to the synthesis of **3a**, particularly its similarity in dimensions to both triostin A and ditercalinium, is vindicated by the finding of a similar mode of binding to DNA. Both of the established bis-intercalators bind around two central base-pairs at a four bp site on the duplex.[28,30] This is crucial as it allows each intercalating group to make a full set of contacts with both bases on either side, a factor demanded by the neighboring site exclusion principle.[11,12,58] The emerging picture for **3a** is of a compound acting like a molecular staple that inserts into the double helix to grip around a two-base pair sandwich. In so doing, interactions are formed with the bases and DNA backbone over a four base pair region. The preferential sequence(s) to which binding of **3a** occurs was investigated by DNase I footprinting experiments. Within the sequence limitations imposed by ∼200 bp of analyzed DNA, it was not possible to determine any exact sequence preference, though it was obvious that impaired cleavage appeared to be more prevalent in regions of mixed sequence rather than runs of a single base or alternating bases. This is implicit in the 5′-TATG-3′ sequence on *tyr*T DNA, the promoter site where binding was observed at the lowest ligand concentration, and in our experiments the most preferred binding site. It has not escaped our notice that this site, along with many of the other footprinted sites, is relatively AT-rich. This is contrary to the classical pattern seen with intercalators, of preferential binding to varied GC-rich areas and low affinity for runs of adenines.[16,24,59] Indeed, most known bis-intercalating compounds have been shown to bind particularly well around CpG or GpC steps.[4,18,28,30,60] Our finding here is supported by the observed preference of MOLRAC compounds in competition dialysis for alternating A−T DNA over natural DNA species and alternating G−C DNA. It may be very significant that the most favored 5′-TATG-3′ sequence in *tyr*T DNA forms part of the TATA box upstream from the transcription start site.

The present results amount to an evaluation of a novel class of DNA-binding compounds and detail the properties of a new sequence-selective bis-intercalator with comparable properties to established drugs such as ditercalinium and echinomycin. Compound **3a** stands apart from established bis-intercalators, both in its novel chemistry and its apparent preference for AT-rich DNA sites. A set of rules for the design of further MOLRAC compounds have been established that can be used to guide the synthesis of a second generation of compounds. Due to the unique properties of the polynorbornane scaffold, the addition of a wide range of functional groups is perfectly possible in further syntheses, providing huge potential for the development of a variety of multifunctional DNA-binding compounds.

Experimental Section

General Procedures and Materials. Purified pUC19 DNA was isolated from XL1-Blue using the Qiagen protocol (Hilden, Germany). Calf thymus topoisomerase I was purchased from Invitrogen and Helena Biosciences. Tris-HCl, Tris-base, EDTA, bovine serum albumin (BSA), phenol/chloroform/isoamyl alcohol (25:24:1), and ethidium bromide were purchased from Sigma-Aldrich. KCl and boric acid were purchased from Riedel de Haën, $MgCl_2$ and bromophenol blue were purchased from BDH, and dithiothreitol (DTT) was purchased from Melford Laboratories. Ultrapure agarose was from GIBCO BRL. Vivaspin 500 concentrators (molecular weight cutoff [MWCO] 30 000) were purchased from Vivascience. Electrophoresis of agarose gels was performed in Owl B2 Gel tanks (CLP) and powered by a Biorad Power Pac 300.

General Synthetic Methods. 1. Reaction between Primary Amines and 9-Chloroacridine. A solution of the relevant amine (1.0 equiv) and 9-chloroacridine (1.0 equiv) in dry DMF or dry DMSO under nitrogen was heated at 125 °C until TLC indicated the reaction to be complete (2.5−5 h), and when cool, the solvent was removed under high vacuum. The residual hydrochloride salt was suspended in DCM (or $CHCl_3$), vigorously stirred, and solubilized as the free base liberated by the dropwise addition of NaOH (40% aqueous solution). The mixture was transferred to a separatory funnel, and the organic phase was washed twice with water, separated, dried ($MgSO_4$), and concentrated in vacuo, leaving a crude product that was subjected to chromatography and/or recrystallized/triturated.

2. ACE Coupling Reactions. One equivalent of both the relevant cyclobutene epoxide and appropriate alkene (two equivalents of alkene are required if a bis-epoxide is used) were dissolved in a minimum amount of solvent (tetrahydrofuran or acetonitrile) and transferred to a thick-walled glass tube that was cooled, sealed, and subsequently heated in an oven at 140 °C for 4−12 h. The tube was cooled and opened, and the contents were subjected to chromatography and/or recrystallization.

3. Ruthenium-Catalyzed [2π+2π] Cycloadditions.[41] A solution of the relevant norbornene (1.0 equiv), dimethyl acetylenedicarboxylate (1.5 equiv), and $RuH_2(CO)(PPh_3)$ (Ru^0) (∼10% w/w norbornene) in benzene was heated at 80 °C until TLC indicated the reaction to be complete. The crude reaction mixture was passed through a short column ($SiO_2/CHCl_3$) to remove the catalyst. The solvent was removed under reduced pressure to afford a crude product that was subsequently purified by chromatography and/or recrystallization.

4. Epoxidation. A solution of the relevant alkene diester (1.0 equiv) dissolved in freshly distilled THF under nitrogen was cooled to 0 °C whereupon TBHP (3.3 M in toluene, 1.5 equiv) was added with stirring. The cold bath was maintained and after 10 min solid KO*t*-Bu (0.3−0.5 equiv) was added in one portion, with vigorous stirring, from a predried, pretared screw cap vial. After a further 15 min, the cold bath was removed and the reaction was allowed to warm to room temperature. When TLC monitoring indicated the reaction to be complete (4−12 h), the reaction was quenched by addition of 10% aqueous Na_2SO_3 (1.5 equiv) and the reaction stirred for a further 10 min. This mixture was subsequently partitioned between DCM/H_2O (or $CHCl_3/H_2O$) and the organic phase was separated. The aqueous phase was extracted twice more with DCM (or $CHCl_3$) and the combined organics were dried ($MgSO_4$), filtered, and concentrated in vacuo. Depending on the purity obtained, the crude product was either subjected to chromatography and/or recrystallized.

5. Deprotection of *tert*-Butyl Carbamates. A solution of the relevant Boc-amine in 20% v/v TFA/DCM (∼1−5 mL for 1 mmol substrate) was stirred at room temperature in a loosely stoppered round-bottom flask. When TLC monitoring indicated the reaction to be complete (12−18 h), the volatiles were removed with gentle heating (30−40 °C) under high vacuum. The residue was redissolved in DCM and transferred to a separatory funnel, where it was washed successively with potassium carbonate (saturated

solution) and brine. The organic phase was separated, dried ($MgSO_4$), filtered, and concentrated in vacuo, leaving pure amine, which was used directly without further purification.

Dimethyl (1a,2b,3a,4a,8a,9a,10b,11a,12b,13a,14a,18a,19a,-20b)-6,16-(2′,2″-Di-(9‴-acridinylamino)ethyl)-6,16-diaza-21-oxaoctacyclo[9.9.1.1.^{3,9}1.^{13,19}0.^{2,10}0.^{4,8}0.^{12,20}0^{14,18}]tricosane-5,7,15,17-tetraone-1,11-dicarboxylate, 3a. Boc-amine **15** (0.15 g, 0.18 mmol) was treated with TFA/DCM (0.5 mL, 20% solution) according to standard method 5. A reaction time of 12 h followed by standard workup provided the intermediate amine as a bright yellow solid that was used without further purification: yield 0.12 g (94%). The reaction of this product (0.12 g, 0.17 mmol) with 9-chloroacridine (0.04 g, 0.17 mmol) in dry DMF (0.8 mL) was performed according to standard method 1. A reaction time of 3.5 h was required, and the crude product was purified by radial chromatography (7.5% MeOH/EtOAc) to provide the title compound as a bright yellow solid: yield 0.09 g (58%), mp 292 °C (dec). ^{1}H NMR (400 MHz, $CDCl_3$): δ 1.12 (2H, d, J = 9.7 Hz, H22a,23a); 1.93 (4H, s, H2,10,12,20); 2.54 (6H, m, H3,9,13,19,-22b,23b); 2.81 (4H, m, H4,8,14,18); 3.44 (4H, m, H1′,1″ or 2′,2″); 3.68 (4H, m, H1′,1″ or 2′,2″); 3.86 (6H, s, OCH_3); 7.25 (4H, m, H2‴,7‴ or 3‴,6‴); 7.53 (4H, m, H2‴,7‴ or 3‴,6‴); 7.81 (4H, m, H1‴,8‴ or 4‴,5‴); 7.95 (4H, d, J = 8.2 Hz, H1‴,8‴ or 4‴,5‴).

Dimethyl (1a,2b,3a,4a,8a,9a,10b,11a,12b,13a,14a,18a,19a,-20b)-6-(4′-(4‴-Acridinyl)-4′-keto-3′-azabutyl)-16-(2″-(9‴-acridinylamino)ethyl)-6,16-diaza-21-oxaoctacyclo [9.9.1.1.^{3,9}1.^{13,19}0.^{2,10}0.^{4,8}0.^{12,20}0^{14,18}]tricosane-5,7,15,17-tetraone-1,11-dicarboxylate, 3b. The alkene **12** (96 mg, 0.25 mmol) and epoxide **20** (102 mg, 0.18 mmol) were combined in a sealed tube with acetonitrile (1.6 mL) and heated (140 °C) for 5 h according to standard method 2. The crude product was purified by radial chromatography (10% MeOH/EtOAc) to yield the title compound as a pale yellow solid: yield 103 mg (60%), mp 198 °C (dec). ^{1}H NMR (400 MHz, $CDCl_3$): δ 1.17 (2H, d, J = 9.3 Hz, H22a,23a); 2.25 (2H, s, H2,10 or 12,20); 2.29 (2H, s, H2,10 or 12,20); 2.58 (2H, m, H3,9 or 13,19); 2.60 (2H, m, H22b,23b); 2.64 (2H, m, H3,9 or 13,19); 2.94 (2H, m, H4,8 or 14,18); 2.97 (2H, m, H4,8 or 14,18); 3.67−3.82 (8H, m, H1′,2′,1′,2″); 3.86 (6H, s, OCH_3); 7.15 (2H, t, J = 9.8 Hz, H2‴″,7‴″ or 3‴″,6‴″); 7.38 (1H, t, J = 10.2 Hz, H2‴″); 7.50 (3H, m, H2‴″,7‴″ or 3‴″,6‴″ and 7‴″); 7.71−7.82 (5H, m, H1‴″,8‴″,6‴″,1‴″,8‴″ or 4‴″,5‴″); 7.88 (2H, d, J = 11.6 Hz, H1‴″,8‴″ or 4‴″,5‴″); 8.10 (1H, d, J = 11.7 Hz, H5‴″); 8.52 (1H, s, H 9‴″); 8.73 (1H, d, J = 9.1 Hz, H 3‴″); 11.93 (1H, s (br), CONH)

Tetramethyl (1a,2b,3a,4b,5a,6a,10a,11a,12b,13a,14b,15a,16b,-17a,18b,19a,20a,24a,25a,26b,27a,28b)-8,22-(2′,2″-Di-(9‴-acridinylamino)-ethyl)-8,22-diaza-30,32-dioxadodecacyclo [13.13.1.1.^{3,13}1.^{5,11}1.^{17,27}1.^{19,25}0.^{2,14}0.^{4,12}0.^{6,10}0.^{16,28}0.^{18,26}0^{20,24}]tritriacontane-7,9,21,23-tetraone-3,13,17,27-tetracarboxylate, 4a. The alkene **12** (0.36 g, 0.95 mmol) and bis-epoxide **28**[26,34,35] (0.19 g, 0.47 mmol) were combined in a sealed tube with acetonitrile (5.5 mL) and heated (140 °C) for 6 h according to standard method 2. The crude product was purified by radial chromatography (10% MeOH/EtOAc) to yield the bis-acridine (**4a**), which was recrystallized (DCM/Pet) as a bright yellow solid: yield 0.22 g (41%), mp 276 °C (dec). ^{1}H NMR (400 MHz, $CDCl_3$): δ 0.31 (4H, s, H2,14,16,28); 1.09 (2H, d, J = 10.2 Hz, H31a,33a); 1.25 (2H, s, H1,15); 1.44 (2H, s, H29); 2.09 (4H, s, H4,12,18,26); 2.49 (4H, s, H5,11,19,25); 2.52 (2H, d, J = 10.2 Hz, H31b,33b); 2.89 (4H, s, H6,10,20,24); 3.70 (12H, s, OCH_3); 4.15 (4H, m, H1′,1″ or 2′,2″); 4.22 (4H, m, H1′,1″ or 2′,2″); 7.39 (4H, t, J = 7.6 Hz, H2‴,7‴ or 3‴,6‴); 7.68 (4H, t, J = 7.6 Hz, H2‴,7‴ or 3‴,6‴); 8.01 (4H, d, J = 7.9 Hz, H1‴,8‴ or 4‴,5‴); 8.09 (4H, d, J = 8.8 Hz, H1‴,8‴ or 4‴,5‴).

Tetramethyl (1a,2b,3a,4b,5a,6b,8a,9b,10a,11b,12a,13b,14a,-15b,16a,17b,19a,20b,21a,22b)-6,17-(2′,2″-Di-(9‴-acridinylamino)ethyl)-24,26-dioxadecacyclo [10.10.1.1.^{3,10}1.^{5,8}1.^{14,21}1.^{16,19}0.^{2,11}0.^{4,9}0.^{13,22}0^{15,20}]heptacosane-3,10,14,21- tetracarboxylates, 4b/c. The alkene **30** (200 mg, 0.64 mmol) and epoxide **28** (130 mg, 0.32 mmol) were combined in a sealed tube with THF (9.0 mL) and heated (140 °C) for 6 h according to standard method 2. The crude products were purified by radial chromatography (5% MeOH/EtOAc) to yield adducts **4b**/**c** as a mixture of isomers (both enantiomers and the *meso*-compound) as a bright yellow solid: yield 179 mg (54%), mp 185−252 °C (dec).

One-Dimensional Unwinding Assay. Each potential intercalator was incubated with pUC19 plasmid (2686 bp) in varying ratios of drug to base pairs (37 °C, 4 h) and relaxed by topoisomerase I (20 units/100 μL total reaction volume) in Tris-HCl, pH 7.5, (50 mM), KCl (50 mM), $MgCl_2$ (10 mM), dithiothreitol (0.5 mM), EDTA (0.1 mM), and bovine serum albumin (200 μg/mL). The reactions were quenched and DNA was extracted with an equal volume of phenol/chloroform:isoamyl/alcohol (25:24:1), removing the protein and ligand. The phases were partitioned by centrifugation (Eppendorf centrifuge 5415- D, 13 000 rcf for 5 min). The top aqueous layer was stored at −80 °C in freezer tubes until analysis was carried out.[61,62,63] Aliquots of 15 μL of each sample were added to 5 μL of loading buffer (20% w/v sucrose, 0.05 M Tris-HCl, pH 7.5, 0.05M EDTA, 50 μg/mL bromophenol blue) and loaded on to 1% (w/v) agarose gels in TBE (80 mM Tris-borate, 1 mM EDTA). Gels were run at 1.9 V/cm (15 h, 600 mL TBE). After electrophoresis, the gels were soaked in TBE and ethidium bromide (1 μg/mL) for 2 h and destained in several changes of water over at least an hour. The gels were then visualized on a GDS-8000 System Transilluminator (UVP Inc., Upland, CA).

Unwinding Angle and Intrinsic Association Constant Determination by Two-Dimensional Gels. Topoisomer separation and subsequent analysis were carried as described by Zeman et al.[50] Circular DNA (pUC19) was relaxed by topoisomerase I in the presence of various concentrations of potential intercalators at a constant ratio of DNA base pair to molecules of ligand. The ligand−DNA mixtures were incubated (37 °C, 4 h) with topoisomerase I (20 units/100 μL total reaction volume) in Tris-HCl, pH 7.5, (50 mM), KCl (50 mM), $MgCl_2$ (10 mM), dithiothreitol (0.5 mM), EDTA (0.1 mM), and bovine serum albumin (200 μg/mL). The reactions were quenched (phenol/chloroform/isoamyl alcohol; vol. ratio 25:24:1), DNA extracted, and stored at −80 °C until gel analysis. For analysis by two-dimensional electrophoresis, samples were thawed and the aqueous phase was concentrated to a volume of approximately 20 μL (Vivaspin concentrator). Aliquots were loaded on to agarose gels (1%) and run as described above. After the first dimension had been run (23 h, TBE, 1.9V/cm), gels were soaked (2 h on a shaker, TBE containing 1.1 μg/mL chloroquine) and rotated 90° before running the second dimension (19 h, TBE + 1.1 μg/mL chloroquine, 1.9V/cm). Gels were stained with ethidium bromide and visualized by UV.

Two-Dimensional Data Analysis. Data were analyzed using Kaleidagraph Software (Synergy Software, Reading, PA). The band intensities for individual topoisomer bands were quantified using Labworks Software (UVP Inc., Upland, CA). The integrated intensities for each topoisomer were plotted to give a Boltzmann distribution from which ΔLk_c was calculated by fitting to the following equation

$$I = I_M \exp[-w(\Delta Lk_c - \Delta Lk_c^0)] \quad (1)$$

I and I_M are, respectively, integrated band intensity and maximum band intensity at the peak of the topoisomer distribution; w is the width of the distribution; and ΔLk_c and ΔLk_c^0 are the average most abundant topoisomer in the Boltzmann population for a reaction with ligand and for the control reaction containing no ligand, respectively. $\phi_{ap,}$, the apparent unwinding angle for each reaction was calculated using

$$\phi_{ap} = 360\left(\frac{N_D}{N_L}\right)(\Delta Lk_c - \Delta Lk_c^0) \quad (2)$$

with N_D equal to the number of plasmid molecules and N_L equal to the number of ligands. The unwinding angle was calculated by fitting the data to

$$\phi_{ap} = \phi - \left[\frac{\phi_{ap}}{(K_a[C_N - (2n-1)C_T)}\right] \quad (3)$$

where n is the neighbor exclusion parameter; C_N and C_T are the concentrations of DNA base pairs and total ligand respectively; and where ϕ_{ap} is the ordinate and $\phi_{ap}/[C_N - (2n\text{-}1)C_T])$ is the abscissa of each binding isotherm. Extrapolating from this equation gives the unwinding angle of the ligand (ϕ) and the ligand association constant (K_a).

Competition Dialysis. The protocol of Ren and Chaires[44] was followed. Briefly, dialysis solution was prepared at 1 μM final concentration in a one liter beaker by adding an appropriate volume of 3 mM stock compound (dissolved in DMSO) to 400 mL of BPES (6 mM Na_2HPO_4, 2 mM NaH_2PO_4, 1 mM EDTA, 185 mM NaCl, pH 7.1). The dialysate concentration was spectrophotometrically verified to be 1 μM using the appropriate molar extinction coefficient for each compound. Molar extinction coefficients (M^{-1} cm^{-1}, with wavelengths) were determined by characterizing the spectra of all compounds in 1% DMSO/99% H_20; **3a** = 12 800 (395 nm), **3b** = 8000 (415 nm), **3c** = 12 000 (410 nm), **3d** = 12 000 (350 nm), **3e** = 18 500 (345 nm), **3f** = 10 500 (345 nm), **4a** = 11 500 (410 nm), **4b**/**c** = 11 500 (420 nm), **12** = 7700 (395 nm). Samples (180 μL) of each polynucleotide (75 μM in BPES) were pipetted into separate 7000 MWCO Pierce Slide-A-Lyzer MINI Dialyzer units, with all eight units then placed in a modified Nalgene plastic float and carefully lowered into the beaker containing the dialysate. Polynucleotide solutions were prepared from commercially available desiccates (Sigma and Amersham Pharmacia). Using a magnetic bar, the dialysate was stirred at 100 rpm at room temperature for 24 h (to equilibrium), with the beaker covered in Parafilm and wrapped in foil to exclude light. Polynucleotide samples were carefully collected from the corner of each dialysis unit and transferred to microcentrifuge tubes. By adding 20 μL of 10% (w/v) sodium dodecyl sulfate (SDS, Sigma) to each sample, a final concentration of 1% (w/v) SDS was created that facilitated the removal of compounds from polynucleotides. Using the appropriate wavelength and extinction coefficient, the concentration of ligand in the dialysate (C_f) was determined against a BPES blank. The total concentration of ligand in each polynucleotide sample (C_t) was then determined by measuring its absorbance against a 1% SDS BPES blank. An appropriate correction for the dilution resulting from the addition of 10% SDS was made. The concentration of drug bound to each polynucleotide (C_b) was then determined by the difference $C_b = C_t - C_f$. From this an apparent binding constant (K_{app}) for ligand−polynucleotide interaction can be calculated using eq 4

$$K_{app} = \frac{C_b}{C_f\,[NA]_{TOTAL}} \tag{4}$$

The $[NA]_{TOTAL}$ refers to the concentration of each nucleic acid sample, in this case maintained at 75 μM. The C_f value was typically set at 1 μM, and thus, K_{app} can be determined simply by dividing the C_b value by 75×10^{-6}. This treatment assumes that potential binding sites are in excess and possible neighbor exclusion effects are neglected. Previous values of K_{app} determined from competition dialysis were found to be in excellent agreement with binding constants obtained from more complete titration studies.[42,43] Measurements were taken using a twin-beam Pye-Unicam SP8−200 UV spectrophotometer accurate to three decimal places. A pair of Hellma quartz cuvettes with a 1 cm light path and a holding volume of 75 μL were used.

DNase I Footprinting. The protocol of Low et al.[64] was used with minor modifications. 3′-End-labeled DNA fragments were prepared for pBS 265mer from the *Eco*RI (Roche) and *Pvu*II (NEB) digestion products of pBS (Stratagene), and for *tyr*T from the *Ava*I (Roche) and *Eco*RI (Roche) digestion products of pAT (a gift from Dr. A. A. Travers, MRC Laboratory of Molecular Biology, University of Cambridge). Digestion products were recovered by ethanol precipitation and then 3′-end-labeled with [α-^{32}P] dATP (NEN/Perkin-Elmer) using AMV reverse transcriptase (Promega). DNA fragments were purified by electrophoresis through a 6% nondenaturing polyacrylamide gel (0.3 mm, 200 V, 2 h in TBE buffer) with resolved radiolabeled DNA fragments visualized by X-ray film imaging. Desired fragments were recovered from corresponding gel regions by excision, crushing, and soaking in 0.4 mL of elution buffer (EB; QIAGEN), with DNA suspensions filtered through 0.8/0.2 μm Acrodisc PF filters (PALL) before being concentrated by ethanol precipitation into a volume of Tris-NaCl buffer (TN: 10 mM Tris, pH 7.4, 10 mM NaCl,) that yields around 200 counts per second per 5 μL of solution (when held up in a pipet tip to a capped Morgan series 900 mini-monitor). Appropriate concentrations of experimental compounds were produced by dilution of a stock solution with TN buffer, and footprinting reactions (overnight incubations at room temperature) were prepared by mixing 4 μL of drug/TN dilution to 2 μL of radiolabeled DNA. Enzymic digestion was initiated by addition at timed intervals of 2 μL of DNase I solution (0.0005 U/mL, Sigma) in DNase I buffer (pH 7.3, 20 mM NaCl, 2 mM $MgCl_2$, 2 mM $MnCl_2$), with digestion stopped after exactly 8 min by the addition of 3 μL of stop solution (formamide containing 10 mM EDTA and 0.1% [w/v] bromophenol blue). Also included were control (Ct) digestions containing no compound and a control not subjected to DNase I cleavage ("uncut"). "G+A" marker tracks were prepared by evaporating 20 μL of water and 5 μL of formamide loading dye (formamide and 0.1% [w/v] bromophenol blue) from 2 μL of radiolabeled DNA at 90 °C for 45 min. Samples were resolved by denaturing polyacrylamide gel electrophoresis (8% acrylamide, 8 M urea, 1× TBE, 0.3 mm thickness, 100 min at 1600 V in 1× TBE) after briefly heating to 90 °C for 4 min and then chilling on wet ice for a further 4 min. Gel images were retrieved with a Molecular Dynamics 425E PhosphorImager after overnight exposure of the dried and fixed gel (treated with 10% acetic acid) to a phosphor storage screen (Molecular Dynamics). For quantitative analysis, gel image scans were transferred to ImageQuant version 3.3 software (Molecular Dynamics) and baseline corrected before being analyzed by integrating all the densities between two selected boundaries. Data were plotted to compare the measured probabilities of cleavage expressed in logarithmic units, $\ln(f_a) - \ln(f_c)$. These units represent the differential cleavage at each bond relative to that in the control (f_a is the fractional cleavage at any bond in the presence of drug and f_c is the fractional cleavage of the same bond in the control). The plotted data were smoothed by taking a three bond running average and displayed on a logarithmic scale for convenience,[64] with each resolved band assigned to a particular bond within the DNA fragment by comparison of its position relative to the sequencing standard (the "G+A" track).

Acknowledgment. We thank Eric Fechter for advice and much-needed help with Zeman−Crothers assays and Marko Hyvonen for help with Scheme 1. T.E. and M.J.W. were supported by grants from the European Union, Cancer Research UK and the Wellcome Trust. T.E. acknowledges the award of a Research Studentship from the MRC. L.D.V. is a Benefactor's Scholar of St. John's College, Cambridge, and was additionally supported by the Cambridge European Trust and the Isaac Newton Trust. F.H. was supported by grants from the MRC and the BBSRC. R.A.R., R.N.W., and P.J.F. acknowledge the support of an Australian Research Council Discovery Grant.

Supporting Information Available: DNase I footprinting analysis of compounds **12** and **4b**/**c**, as in Figure 5, and a comparison of divalent intercalators **3a**, **4a**, **4b**/**c**, **3b**, **3c**, **3d**, **3e**, and **3f** in a one-dimensional unwinding assay, as in Figure 1; analytical and additional spectral data for all new compounds described above; ^{13}C NMR data for key compounds **3a**, **3b**, and **4a**; and synthetic methods and spectral data for all intermediate and biologically inactive compounds. This material is available free of charge via the Internet at http://pubs.acs.org.

References

(1) Acheson, R. M. ed. *Acridines*, 2nd ed.; Wiley: London, 1973.
(2) Albert, A. *Selective Toxicity*, 5th ed.; Chapman & Hall: London, 1973.

(3) Bischoff, G.; Hoffmann, S. DNA-binding of drugs used in medicinal therapies. *Curr. Med. Chem.* **2002**, *9*, 312−348.
(4) Waring, M. J.; Bailly, C. DNA recognition by intercalators and hybrid molecules. *J. Mol. Recognit.* **1994**, *7*, 109−122.
(5) Berge, T.; Jenkins, N. S.; Hopkirk, R. B.; Waring, M. J.; Edwardson, J. M.; et al. Structural perturbations in DNA caused by bis-intercalation of ditercalinium visualised by atomic force microscopy. *Nucleic Acids Res.* **2002**, *30*, 2980−2986.
(6) Dervan, P. B.; Burli, R. W. Sequence-specific DNA recognition by polyamides. *Curr. Opin. Chem. Biol.* **1999**, *3*, 688−693.
(7) Thurston, D. E. Nucleic acid targeting: therapeutic strategies for the 21st century. *Br. J. Cancer* **1999**, *80* (Suppl 1), 65−85.
(8) Lerman, L. S. Structural considerations in the interaction of DNA and acridines. *J. Mol. Biol.* **1961**, *3*, 18−30.
(9) Chaires, J. B. Drug−DNA interactions. *Curr. Opin. Struct. Biol.* **1998**, *8*, 314−320.
(10) Wainwright, M. Acridine-a neglected antibacterial chromophore. *J. Antimicrob. Chemother.* **2001**, *47*, 1−13.
(11) Wakelin, L. P. G.; Romanos, M.; Chen, T. K.; Glaubiger, D.; Canellakis, E. S.; et al. Structural limitations on the bifunctional intercalation of diacridines into DNA. *Biochemistry* **1978**, *17*, 5057−5063.
(12) Gale, E. F.; Cundliffe, E.; Reynolds, P. E.; Richmond, M. H.; Waring, M. J. *The Molecular Basis of Antibiotic Action*, 2nd ed.; Wiley: London, 1981.
(13) Wakelin, L. P. G.; Adams, A.; Denny, W. A. Kinetic studies of the binding of acridinecarboxamide topoisomerase poisons to DNA: Implications for mode of binding of ligands with uncharged chromophores. *J. Med. Chem.* **2002**, *45*, 894−901.
(14) Denny, W. A. Acridine derivatives as chemotherapeutic agents. *Curr. Med. Chem.* **2002**, *9*, 1655−1665.
(15) Wakelin, L. P. G.; Creasy, T. S.; Waring, M. J. Equilibrium constants for the binding of an homologous series of monofunctional and bifunctional intercalating diacridines to calf thymus DNA. *FEBS Lett.* **1979**, *104*, 261−265.
(16) Waring, M. J.; Wakelin, L. P. G. Echinomycin: A bifunctional intercalating antibiotic. *Nature* **1974**, *252*, 653−657.
(17) Wright, R. G.; Wakelin, L. P. G.; Fieldes, A.; Acheson, R. M.; Waring, M. J. Effects of ring substituents and linker chains on the bifunctional intercalation of diacridines into deoxyribonucleic acid. *Biochemistry* **1980**, *19*, 5825−5836.
(18) Bailly, C.; Braña, M.; Waring, M. J. Sequence-selective intercalation of antitumour bis-naphthalimides into DNA. Evidence for an approach via the major groove. *Eur. J. Biochem.* **1996**, *240*, 195−208.
(19) Mammen, M.; Choi, S. K.; Whitesides, G. M. Polyvalent interactions in biological systems: Implications for design and use of multivalent ligands and inhibitors. *Angew. Chem., Int. Ed.* **1998**, 2755−2799.
(20) Page, M. I.; Jencks, W. P. Entropic rate accelerations in enzymic and intramolecular reactions and the chelate effect. *Proc. Natl. Acad. Sci. U.S.A.* **1971**, *68*, 1678−1683.
(21) Bailly, C.; Carrasco, C.; Joubert, A.; Bal, C.; Wattez, N.; et al. Chromophore-modified bisnaphthalimides: DNA recognition, topoisomerase inhibition, and cytotoxic properties of two mono- and bisfuronaphthalimides. *Biochemistry* **2003**, *42*, 4136−4150.
(22) Crothers, D. M.; Sabol, S. L.; Ratner, D. I.; Müller, W. Studies concerning the behavior of actinomycin in solution. *Biochemistry* **1968**, *7*, 1817−1823.
(23) Denny, W. A.; Atwell, G. J.; Baguley, B. C.; Wakelin, L. P. G. Synthesis and antitumor activity of new classes of diacridines: Importance of linker chain rigidity for DNA binding kinetics and biological activity. *J. Med. Chem.* **1985**, *28*, 1568−1574.
(24) Wakelin, L. P. G.; Chetcuti, P.; Denny, W. A. Kinetic and equilibrium binding studies of amsacrine-4-carboxamides: A class of asymmetrical DNA-intercalating agents which bind by threading through the DNA helix. *J. Med. Chem.* **1990**, *33*, 2039−2044.
(25) Warrener, R. N.; Butler, D. N.; Liu, L.; Margetic, D.; Russell, R. A. Incorporation of a molecular hinge into molecular tweezers by using tandem cycloadditions onto 5,6-dimethylenenorbornene. *Chemistry* **2001**, *7*, 3406−3414.
(26) Warrener, R. N.; Butler, D. N.; Russell, R. A. *Synlett* **1998**, 566-573.
(27) Warrener, R. N.; Butler, D. N.; Golic, M. The synthesis of geometric variants of rigidly-linked uracil-{spacer}-uracil and uracil-{spacer}-effector molecules using BLOCK assembly methods. *Nucleosides Nucleotides* **1999**, *18*, 2631−2660.
(28) Gao, Q.; Williams, L. D.; Egli, M.; Rabinovich, D.; Chen, S. L.; et al. Drug-induced DNA repair: X-ray structure of a DNA−ditercalinium complex. *Proc. Natl. Acad. Sci. U.S.A.* **1991**, *88*, 2422−2426.
(29) Addess, K. J.; Feigon, J. Sequence specificity of quinoxaline antibiotics. 1. Solution structure of a 1:1 complex between triostin A and [d(GACGTC)]2 and comparison with the solution structure of the [N-MeCys3,N-MeCys7]TANDEM-[d(GATATC)]2 complex. *Biochemistry* **1994**, *33*, 12386−12396.
(30) Ughetto, G.; Wang, A. H.; Quigley, G. J.; van der Marel, G. A.; van Boom, J. H.; et al. A comparison of the structure of echinomycin and triostin A complexed to a DNA fragment. *Nucleic Acids Res.* **1985**, *13*, 2305−2323.
(31) *MM2 embedded into Chem3D*, 7.0 ed., 2001; CambridgeSoft: Cambridge.
(32) Pfeffer, F. M.; Russell, R. A. Strategies and methods for the attachment of amino acids and peptides to chiral [*n*]polynorbornane templates. *Org. Biomol. Chem.* **2003**, *1*, 1845−1851.
(33) Butler, D. N.; Hammond, M. L.; Johnston, M. R.; Sun, G.; Malpass, J. R.; et al. In-line proximity effects in extended 7-azanorbornanes. 1. A new concept for modifying effector group separation based on the control of *N*-invertomer geometry. *Org. Lett.* **2000**, *2*, 721−724.
(34) Warrener, R. N.; Schultz, A. C.; Bulter, D. N.; Mahadavan, I. B.; Russell, R. A. *J. Chem. Soc., Chem. Commun.* **1997**, 1023−1024.
(35) Warrener, R. N.; Margetic, D.; Foley, P. J.; Butler, D. N.; Winling, A.; et al. *Tetrahedron Lett.* **2000**, *51*, 571.
(36) Mitsudo, T.; Kokuryo, K.; Shinsugy, T.; Nakagawa, Y.; Takegami, Y. *J. Org Chem.* **1979**, *44*, 4492−4496.
(37) Mitsudo, T.; Naruse, H.; Kondo, T.; Ozaki, Y.; Watanabe, Y. *Angew. Chem., Int. Ed. Engl.* **1994**, *33*, 580−581.
(38) Seitz, V. G.; Wassmuth, H. *Chem.-Ztg.* **1988**, *112*, 80−81.
(39) Warrener, R. N.; Butler, D. N.; W. Y., L.; Pitt, I. G.; Russell, R. A. *Tetrahedron Lett.* **1991**, *32*, 1889−1892.
(40) Warrener, R. N.; Butler, D. N.; Margetic, D. N.; Pfeffer, F. M.; Russell, R. A. *Tetrahedron Lett.* **2000**, *41*, 4671−4675.
(41) Holmes, H. L. The Diels Alder Reaction. Ethylenic and Acetylenic Dienophiles. *Organic Reactions*; Wiley: New York, 1967; pp 60−173.
(42) Ren, J.; Jenkins, T. C.; Chaires, J. B. Energetics of DNA intercalation reactions. *Biochemistry* **2000**, *39*, 8439−8447.
(43) Ren, J.; Bailly, C.; Chaires, J. B. NB-506, an indolocarbazole topoisomerase I inhibitor, binds preferentially to triplex DNA. *FEBS Lett.* **2000**, *470*, 355−359.
(44) Ren, J.; Chaires, J. B. Rapid screening of structurally selective ligand binding to nucleic acids. *Methods Enzymol.* **2001**, *340*, 99−108.
(45) Chaires, J. B., personal communication.
(46) Ren, J.; Chaires, J. B. Sequence and structural selectivity of nucleic acid binding ligands. *Biochemistry* **1999**, *38*, 16067−16075.
(47) Zeman, S. M.; Crothers, D. M. Simultaneous measurement of binding constants and unwinding angles by gel electrophoresis. *Methods Enzymol.* **2001**, *340*, 51−68.
(48) Dias, N.; Jacquemard, U.; Baldeyrou, B.; Tardy, C.; Lansiaux, A.; et al. Targeting DNA with novel diphenylcarbazoles. *Biochemistry* **2004**, *43*, 15169−15178.
(49) Dias, N.; Goossens, J. F.; Baldeyrou, B.; Lansiaux, A.; Colson, P.; et al. Oxoazabenzo[de]anthracenes conjugated to amino acids: Synthesis and evaluation as DNA-binding antitumor agents. *Bioconjugate Chem.* **2005**, *16*, 949−958.
(50) Zeman, S. M.; Depew, K. M.; Danishefsky, S. J.; Crothers, D. M. Simultaneous determination of helical unwinding angles and intrinsic association constants in ligand−DNA complexes: The interaction between DNA and calichearubicin B. *Proc. Natl. Acad. Sci. U.S.A.* **1998**, *95*, 4327−4332.
(51) Galas, D. J.; Schmitz, A. DNAse footprinting: A simple method for the detection of protein−DNA binding specificity. *Nucleic Acids Res.* **1978**, *5*, 3157−3170.
(52) Fox, K. R. DNase I footprinting. *Methods Mol. Biol.* **1997**, *90*, 1−22.
(53) Bailly, C.; Kluza, J.; Martin, C.; Ellis, T.; Waring, M. J. DNase I footprinting of small molecule binding sites on DNA. *Methods Mol. Biol.* **2005**, *288*, 319−342.
(54) Crow, S. D.; Bailly, C.; Garbay-Jaureguiberry, C.; Roques, B.; Shaw, B. R.; et al. DNA sequence recognition by the antitumor drug ditercalinium. *Biochemistry* **2002**, *41*, 8672−8682.
(55) Goodisman, J.; Dabrowiak, J. C. Structural changes and enhancements in DNase I footprinting experiments. *Biochemistry* **1992**, *31*, 1058−1064.
(56) Pfeffer, F. unpublished observations.
(57) Fechter, E. J.; Dervan, P. B. Allosteric inhibition of protein−DNA complexes by polyamide−intercalator conjugates. *J. Am. Chem. Soc.* **2003**, *125*, 8476−8485.
(58) Bresloff, J. L.; Crothers, D. M. Equilibrium studies of ethidium−polynucleotide interactions. *Biochemistry* **1981**, *20*, 3547−3553.
(59) Lokey, R. S.; Kwok, Y.; Guelev, V.; Pursell, C. J.; Hurley, L. H.; et al. A new class of polyintercalating molecules. *J. Am. Chem. Soc.* **1997**, *119*, 7202−7210.

(60) Leng, F.; Priebe, W.; Chaires, J. B. Ultratight DNA binding of a new bisintercalating anthracycline antibiotic. *Biochemistry* **1998**, *37*, 1743−1753.
(61) Keller, W. Determination of the number of superhelical turns in simian virus 40 DNA by gel electrophoresis. *Proc. Natl. Acad. Sci. U.S.A.* **1975**, *72*, 4876−4880.
(62) Bailly, C.; O'Huigin, C.; Houssin, R.; Colson, P.; Houssier, C.; et al. DNA-binding properties of a distamycin-ellipticine hybrid molecule. *Mol. Pharmacol.* **1992**, *41*, 845−855.
(63) OhUigin, C.; McConnell, D. J.; Kelly, J. M.; van der Putten, W. J. Methylene blue photosensitised strand cleavage of DNA: Effects of dye binding and oxygen. *Nucleic Acids Res.* **1987**, *15*, 7411−7427.
(64) Low, C. M.; Olsen, R. K.; Waring, M. J. Sequence preferences in the binding to DNA of triostin A and TANDEM as reported by DNase I footprinting. *FEBS Lett.* **1984**, *176*, 414−420.

JM0613020